Technische Universität Berlin
Institut für Mathematik

The Honigmann Process - a mathematical study

Ann-Kristin Baum*, **Lia Strenge***

Preprint 2015-04

Preprint-Reihe des Instituts für Mathematik
Technische Universität Berlin
http://www.math.tu-berlin.de/preprints

Report 2015-04 **April 2015**

The Honigmann Process - a mathematical study

Ann-Kristin Baum*, Lia Strenge*

April 11, 2015

Abstract

The Honigmann process is a thermochemical energy storage converting low temperature heat into mechanical work. To control and optimize the operation of the storage, the Honigmann process is simulated numerically using a set of differential-algebraic equations (DAEs) as governing equations. We analyze this DAE regarding its solvability, the uniqueness of solutions and the efficiency of numerical solvers. We identify the steps of the process modeled by a reliable, uniquely solvable mathematical model and point out those steps, where the mathematical model may lead to ambiguous solutions. For the steps of the process described by a uniquely solvable model, we compare several numerical solvers with respect to efficiency and accuracy.

Keywords: Thermochemical Energy Storage, Honigmann Process, Strangeness Index, Differential-Algebraic Equations

AMS(MOS) subject classification:

1 Introduction

One main barrier for the dissemination of renewable energies are insufficient energy storage technologies [59]. Contributing to the efforts to overcome this barrier, cp. e.g. [1], [63, p. 163ff.], the *Honigmann process* has been proposed in [31], [32] for, e.g., a medium-size industrial application where low temperature heat is available. The Honigmann process is a thermochemical energy storage based on absorption that converts low-temperature heat into mechanical work. To charge the process, heat that is available, e.g. as industrial waste heat, is used to evaporate water from a salt solution and thus to concentrate the solution. To recover the stored energy, the vapor pressure depression over the salt solution is used to drive a steam engine. The process was first developed in the 19th century as 'fireless locomotive' [28, 27] and it is currently build and analyzed anew in a DFG project at the TU Berlin [31, 32].
To simulate, control and optimize the operation of the storage, the Honigmann process is modeled mathematically using a sequence of non-linear differential-algebraic equations (DAEs) [33, 64]. DAEs model dynamic processes that are restricted in their evolution by additional algebraic constraints, like joints in multibody systems, cp. e.g. [16, 58, 60, 61], connections and loops in electrical circuits or networks, cp. e.g. [17, 65] or balance equations and conservation laws in

*Institut für Mathematik, TU Berlin, Straße des 17. Juni 136, 10623 Berlin, Germany.
baum@math.tu-berlin.de, liast@posteo.de
The authors have been supported by *European Research Council* through ERC Advanced Grant "Modeling, Simulation and Control of Multi-Physics Systems" MODSIMCONMP.

biological and chemical systems, see e.g. [29]. The sequential modeling is physically motivated as the structure of the machinery changes during the operation, cp. Section 2. The mathematical models considered here have been validated and tested in [33] and [64] for selected initial values and parameter scenarios using the modeling software Dymola. To generalize these results onto the full domain of definition of each DAE model and to specify these domains, we study the solvability and uniqueness of solutions using the concept of the strangeness-index [35, 36, 37, 38]. We identify the model associated with the discharging of the storage as a well-posed DAE having unique solutions for every consistent initial value. We remodel these equations such that they allow for a simulation with standard simulators provided by MATLAB and compare the performance and accuracy of these solvers with the DAE solvers DASSL [51] and the code GENDA developed at TU Berlin [40] . For the models associated with the charging step and the transition phases between charging and discharging, we point out problems regarding the existence and uniqueness of solutions and how these problems may be solved by remodeling the system.

2 The Honigmann process

Explaining the physical process and the operation of the Honigmann process in Section 2.1, we derive the modeling equations serving as mathematical model in Section 2.2.

2.1 The physical process

The Honigmann process as studied in [31] consists of two separated tanks, one of which filled with water, called the working fluid, the other one containing the solution, here Lithium Bromide, see Figure 2.1. To charge the storage, the two tanks are connected by a valve. To discharge the storage, the tanks are connected by a turbine and a heat exchanger. In order to study the overall energy balance and to be able to define the efficiency, the Honigmann process is modeled as a cyclic process.

Assuming that the storage has been charged, i.e., that the salt solution has been concentrated and the tanks are kept at a same or similar temperature, the vapor pressure depression over the solution compared to the working fluid leads to a pressure difference between both fluids. This pressure difference induces a vapor flow of the working fluid into the solution tank. Connecting the tanks by a turbine, then parts of the thermochemical energy can be converted to mechanical work, or, adding a generator, to electrical work. Connecting the tanks with a heat exchanger, the heat of absorption of the working fluid in the salt solution can be led back to the solution tank to feed further evaporation of the working fluid. This *discharging* of the process continues until the pressure difference between the two tanks is balanced, i.e., until the dilution of the salt solution is such that the pressure depression over the solution is too small to induce a further vapor flow. In operation, the process may be terminated as soon as the power of the turbine drops below a given threshold or a predefined final salt concentration is reached. The set up of the discharging step is illustrated in Figure 2.1, left.

To charge the process again, the heat exchanger is removed and the turbine is replaced by a valve, cp. Figure 2.1, right. Closing the valve, the tanks are first heated or cooled separately to balance the pressure. Opening the valve again, the solution is concentrated by heating the solution tank using low temperature heat available, e.g. from industrial waste heat or a solar collector, and cooling the working fluid tank on ambient temperature level. Hence, the charging step is modeled as an *isobare desorption*. To obtain a cyclic process, the solution is concentrated

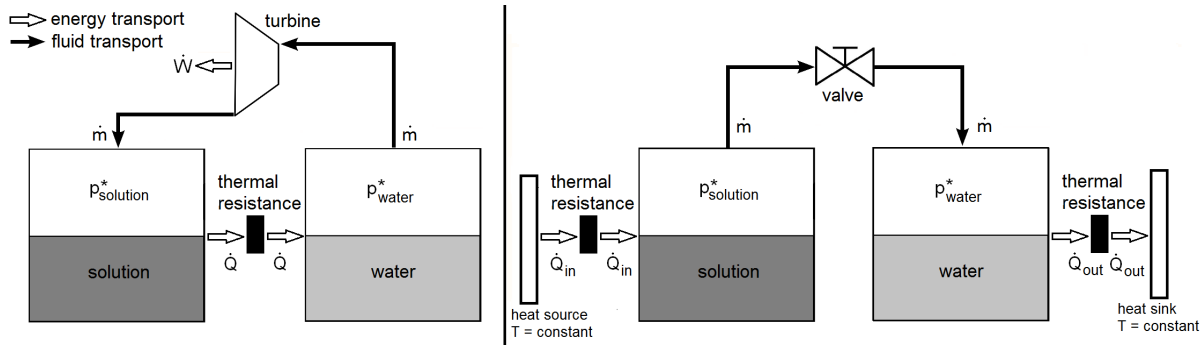

Figure 2.1: Discharge and charge of the Honigmann storage

to its initial concentration of the discharging step. Closing the valve again, also the tanks are brought to their initial temperatures.

2.2 The mathematical model

To derive the mathematical model for the Honigmann process as described in Section 2.1, we specify the assumptions on the testing plant, cp. [64, p. 9ff.]. We assume that the tanks are closed and we assume that only the liquid phases are contained, i.e., there is no vapour volume within the tanks and we only consider the vapour pressure of the liquids. Following [64, p. 9ff.], we assume that in both tanks the specific inner energy u approximately equals the specific enthalpy h, allowing to neglect $p \cdot v$, i.e., the product of pressure p and specific volume v. The working fluid and the solution are given by water and Lithium Bromide/water solution, respectively. As a common assumption for aqueous liquids according to the incompressible substance model, [47, p. 93f.], we assume that these fluids are incompressible, i.e. have a constant density independent of the pressure. The tanks are connected by a turbine and a valve, to convert the thermochemical energy into mechanical work and to disconnect the two tanks in the discharging/charging step, respectively. The turbine produces mechanical work. Adding a generator, also electrical energy can be generated. Thermically, the tanks are connected by a heat transfer circuit ensuring a uniform temperature distribution in the individual tanks.

2.2.1 The discharging step

The mathematical model is based on the energy and mass balances of the individual components. For the working fluid we have that

$$H_w = m_w h_w, \tag{2.1a}$$
$$\dot{H}_w = Q_{flow} - m_{flow} h_{v,w}, \tag{2.1b}$$
$$\dot{m}_w = -m_{flow}, \tag{2.1c}$$

and for the solution, we obtain analogously

$$H_{sol} = m_{sol} h_{sol}, \tag{2.1d}$$
$$\dot{H}_{sol} = -Q_{flow} + m_{flow} h_{v,sol}, \tag{2.1e}$$
$$\dot{m}_{sol} = m_{flow}, \tag{2.1f}$$

where H_w, H_{sol}, h_w, h_{sol} and m_w, m_{sol} are the (specific) enthalpies and masses of the water and the solution, respectively, and Q_{flow}, m_{flow} are the heat and mass flow between the tanks. Outside the wet steam area, the specific enthalpies $h_{l,fluid}, h_{v,fluid}$ of the liquid and vapor phase of a given fluid are specified by two specific properties of the fluid, like temperature and pressure, temperature *or* pressure and specific entropy, temperature *or* pressure and specific volume, see [26, 2]. Assuming that both fluids and the vapor are in equilibrium state, the specific enthalpies h_w, $h_{v,w}$, $h_{v,sol}$ are uniquely determined by the temperature *or* the pressure - and the salt concentration for h_{sol} [2]. Hence, for the water tank we obtain

$$p_w = f_1(T_w), \tag{2.1g}$$
$$h_w = f_2(T_w), \tag{2.1h}$$
$$h_{v,w} = f_3(T_{v,w}), \tag{2.1i}$$

where T_w, $T_{v,w}$ are the temperatures of the water fluid and vapor, respectively, and p_w its pressure. Accordingly, for the solution, we have that

$$T_{v,sol} = f_6(h_{v,sol}, p_{sol}), \tag{2.1j}$$
$$p_{sol} = f_7(T_{sol}, X_{salt}), \tag{2.1k}$$
$$h_{sol} = f_8(T_{sol}, X_{salt}), \tag{2.1l}$$

where T_{sol}, $T_{v,sol}$ are the temperatures of the solution fluid and vapor, respectively, and p_{sol} its pressure. The functions f_1, f_2, f_3 and f_6, f_7, f_8 are implicitly given in terms of experimental data, fitted curves or coefficient tables, see [30] and [50]. However, as the relation of h, p, T and X is unique, the functions $f_1, f_2, f_3, f_6, f_7, f_8$ can be assumed to be invertible in every argument. Numerically, this is realized using Newton's method. In particular, as h, p, T and X are positive, $f_1, f_2, f_3, f_6, f_7, f_8$ and their inverse functions are positive on their domain of definition.
For the working tank, we assume that the water and the vapor stream have the same temperature, i.e.,

$$T_{v,w} = T_w. \tag{2.1m}$$

For the solution, the current concentration X_{salt} is given by

$$X_{salt} = \frac{m_{salt}}{m_{sol}}, \tag{2.1n}$$

where the amount of salt m_{salt} in the solution tank is constant and determined by the initial conditions, see Section 4.2. For the turbine, the power P_m is proportional to the enthalpy difference of the vapor stream passing through the turbine, i.e.,

$$P_m = |m_{flow}| \cdot (h_{v,in,w} - h_{v,out,sol}), \tag{2.1o}$$

where $h_{v,out,sol}$, $h_{v,in,w}$ are the enthalpies of the vapor on the solution and the water side, respectively, and m_{flow} denotes the mass flow through the turbine. The mass flow rate m_{flow} is modeled by the Stodola equation which is used for turbines in part load operations, see [34], i.e.,

$$\frac{m_{flow}^2}{K} = p_{in,w}^2 - p_{out,sol}^2, \tag{2.1p}$$

where $K = \frac{m_{flow,N}^2}{p_{in,N}^2 - p_{out,N}^2}$ is a constant containing the nominal values with index N. The nominal mass flow rate $m_{flow,N}$ should be chosen as the maximal mass flow rate which results from the

maximal pressure difference, i.e. maximal occurring inlet pressure, minimal occurring outlet pressure [64, p. 14]. The enthalpy difference $h_{v,out,sol} - h_{v,in,w}$ can be computed from the *isentropic efficiency* $\eta_{isentropic}$ of the turbine which denotes the ratio of the actual and the ideal work, i.e.,

$$\eta_{isentropic} = \frac{h_{v,in,w} - h_{v,out,sol}}{h_{v,in,w} - h_{v,out,isen}}. \tag{2.1q}$$

The enthalpy $h_{v,out,isen}$ at the outlet state is given by

$$h_{v,out,isen} = f_5\left(s_v, p_{sol}\right), \tag{2.1r}$$

where p_{sol} is the pressure of the solution fluid and s_v is the specific entropy of the vapor. The entropy s_v is computed from the enthalpy $h_{v,w}$ and the pressure of the working fluid p_w, i.e.,

$$s_v = f_4\left(h_{v,w}, p_w\right). \tag{2.1s}$$

The functions f_4, f_5 are taken from [26] using the propery library for water [30]. The heat flow Q_{flow} between the tanks is proportional to the temperature drop $T_{sol} - T_w$ of the solution and the working fluid, i.e.,

$$Q_{flow} = G(T_{sol} - T_w), \tag{2.1t}$$

where G is the thermal conductance. The total heat which is transfered from the solution tank to the working fluid tank is given by the integral over the heat flow rate:

$$\dot{Q} = Q_{flow}, \tag{2.1u}$$

In conclusion, the discharging step is modeled by the equations (2.1) to which we refer as

$$0 = F_{dch}\left(t, x, \dot{x}\right),$$

where $F_{dch}\colon \mathbb{D}_{dch} \to \mathbb{R}^{21}$ is a function on a suitable open set $\mathbb{D}_{dch} = \mathcal{I}_{dch} \times \Omega_{x,dch} \times \Omega_{\dot{x},dch}$ in $\mathbb{R} \times \mathbb{R}^{21} \times \mathbb{R}^{21}$.
The function F_{dch} and its variable x are summarized with their physical units in Section 4.2.

2.2.2 The charging step

For the charging step, the turbine is replaced by a valve and the thermal connection between the tanks is interrupted, such that each tank can be cooled or heated separately. Still, the assumptions concerning, e.g., the internal energy and incompressibility stated in Section 2.2.1 remain valid, see [64, p. 9ff.].
Due to the hybrid, i.e. switching, behaviour of the valve (open/closed) leading to different relations of pressure, specific enthalpy and mass flow rate between the tanks, in [64] the charging step is modeled sequentially in three distinct sets of equations. This avoids events during the simulation. The actual isobare desorption is described by the second model, while the first and last one model the transition phases in which the system is steered into the initial state for the desorption and absorption, respectively. The cyclic boundary conditions are necessary to quantify properties like efficiency and energy density.

2.2.3 Charging part II: Isobare Desorption with open valve

Like for the discharging step, the model for the charging is based on the energy and mass balances of the individual components. For the water, we have that

$$H_w = m_w h_w, \tag{2.2a}$$
$$\dot{H}_w = Q_{flow,w} - m_{flow} h_{v,w}, \tag{2.2b}$$
$$\dot{m}_w = -m_{flow}, \tag{2.2c}$$

and for the solution, we obtain analogously

$$H_{sol} = m_{sol} h_{sol}, \tag{2.2d}$$
$$\dot{H}_{sol} = -Q_{flow,sol} + m_{flow} h_{v,sol}, \tag{2.2e}$$
$$\dot{m}_{sol} = m_{flow} \tag{2.2f}$$

where H_w, H_{sol}, h_w, h_{sol} and m_w, m_{sol} are the (specific) enthalpies and masses of the water and the solution, respectively, and Q_{flow}, m_{flow} are the heat and mass flow between the tanks. As in Section 2.2.1, we assume that the working fluid and vapor are in phase equilibrium and thus get that

$$p_w = f_1(T_w), \tag{2.2g}$$
$$h_w = f_2(T_w), \tag{2.2h}$$
$$T_{v,w} = f_6(h_{v,w}, p_w), \tag{2.2i}$$

where T_w, $T_{v,w}$ are the temperatures of the water and vapor, respectively, and p_w its pressure. Accordingly, for the solution, we have that

$$h_{v,sol} = f_3(T_{v,sol}), \tag{2.2j}$$
$$p_{sol} = f_7(T_{sol}, X_{salt}), \tag{2.2k}$$
$$h_{sol} = f_8(T_{sol}, X_{salt}), \tag{2.2l}$$

where T_{sol}, $T_{v,sol}$ are the temperatures of the solution and the vapor, respectively, and p_{sol} its pressure. For the solution tank, we assume that the vapor stream has the same temperature as the liquid, i.e., we have that

$$T_{v,sol} = T_{sol}. \tag{2.2m}$$

The Lithium Bromide concentration X_{Salt} is given by

$$X_{salt} = \frac{m_{salt}}{m_{sol}}, \tag{2.2n}$$

where the amount of salt m_{salt} in the solution tank is constant. During the desorption, the open valve connects the tanks isenthalpically and without loss of pressure and we get the equations

$$h_{v,w} = h_{v,sol}, \tag{2.2o}$$
$$p_w = p_{sol}. \tag{2.2p}$$

The heat flow Q_{flow} between the tanks and the corresponding temperature source is proportional to the temperature difference, i.e., we have that

$$Q_{flow,sol} = G_{sol} \cdot (T_{sol} - T_{q,sol}), \tag{2.2q}$$
$$Q_{flow,w} = G_w \cdot (T_w - T_{q,w}), \tag{2.2r}$$

where G_{sol} and G_w are thermal conductances. The total heat which is transferred to or from each tank is given by

$$\dot{Q}_{sol} = Q_{flow,sol}, \tag{2.2s}$$
$$\dot{Q}_w = Q_{flow,w}. \tag{2.2t}$$

In conclusion, the charging step is modeled by the equations (2.2) to which we refer as

$$0 = F_{ch}\left(t, x, \dot{x}\right),$$

where $F_{ch}\colon \mathbb{D}_{ch} \to \mathbb{R}^{20}$ is a function on a suitable open set $\mathbb{D}_{ch} = \mathcal{I}_{ch} \times \Omega_{x,ch} \times \Omega_{\dot{x},ch}$ in $\mathbb{R} \times \mathbb{R}^{20} \times \mathbb{R}^{20}$.
The function F_{dch} and its variable x are summarized with their physical units in Section 4.2.

2.2.4 Charging part I and III: Heating and Cooling with closed valve

In the transitions phases between charging and discharging in which the pressure and temperature of the tanks are balanced and brought to the respective initial values, the valve connecting the two tanks is closed. Equations (2.2i), (2.2o), (2.2p) are replaced by

$$h_{v,w} = f_3\left(T_{v,w}\right), \tag{2.3i}$$
$$m_{flow} = 0, \tag{2.3o}$$
$$T_{v,w} = T_w, \tag{2.3p}$$

while the other equations in (2.2) are preserved. Denoting these equations by (2.3a) to (2.3t), respectively, the intermediate steps are modeled by the equations (2.3) to which we refer as

$$0 = F_{int}\left(t, x, \dot{x}\right),$$

where $F_{int}\colon \mathbb{D}_{int} \to \mathbb{R}^{20}$ is a function on a suitable open set $\mathbb{D}_{int} = \mathcal{I}_{int} \times \Omega_{x,int} \times \Omega_{\dot{x},int}$ in $\mathbb{R} \times \mathbb{R}^{20} \times \mathbb{R}^{20}$.

3 The Strangeness Index of the Honigmann process

The Honigmann process as modeled in (2.1), (2.2) and (2.3) is a sequence of coupled differential and algebraic equations, DAEs. DAEs have been widely studied in, e.g., [6, 8, 9, 10, 11, 12, 13, 14, 18, 19, 20, 21, 22, 23, 42, 43, 44, 49, 54, 55, 56, 57] and the references therein. To illustrate the difficulties arising from the coupling of differential and algebraic equations, we consider the semi-explicit, consistent initial value problem

$$\dot{x}_1 = f(t, x_1, x_2), \qquad x_1(t_0) = x_{1,0}, \tag{3.1a}$$
$$0 = g(t, x_1, x_2), \qquad g(t_0, x_{1,0}, x_{2,0}) = 0. \tag{3.1b}$$

If $g_{x_2}(t_0, x_{1,0}, x_{2,0})$ is nonsingular, then by the Implicit Function Theorem [48], the algebraic equation (3.1b) is uniquely solvable for x_2 in a neighborhood of $(t_0, x_{1,0}, x_{2,0})$ and the solution is given by $x_2 = \hat{g}(t, x_1)$ for a suitable function $\hat{g}$. Inserting this solution into the differential equation (3.1a) and setting $\hat{f}(t, x_1) := f(t, x_1, \hat{g}(t, x_1))$, we obtain an ODE depending on x_1 only. If $\hat{f}$ is locally Lipschitz, then there exists a unique solution of this ODE [5]. Hence, the (3.1) is uniquely solvable if $g_{x_2}(t_0, x_{1,0}, x_{2,0})$ nonsingular and f, g are sufficiently smooth.
If $g_{x_2}(t_0, x_{1,0}, x_{2,0})$ is singular, then the algebraic equation (3.1b) may not be (uniquely) solvable. Consequently, the DAE (3.1) may not be (uniquely solvable). Furthermore, the DAE contains hidden constraints and may pose stricter smoothness assumptions on input functions than are available. To illustrate these issues, we differentiate the algebraic equation (3.1b) and obtain that

$$0 = g_{x_1}\dot{x}_1 + g_{x_2}\dot{x}_2 + g_t. \tag{3.2}$$

As $g_{x_2}(t_0, x_{1,0}, x_{2,0})$ is singular, there exists a matrix U_2 such that $(U_2 g_{x_2})(t_0, x_{1,0}, x_{2,0}) = 0$. Then, a solution of (3.1) must satisfy

$$0 = (U_2^T g_{x_1})(t_0, x_{1,0}, x_{2,0})\dot{x}_1(t_0) + (U_2^T g_t)(t_0, x_{1,0}, x_{2,0}). \tag{3.3}$$

$$0 = (U_2^T g_{x_1} f)(t_0, x_{1,0}, x_{2,0}) + (U_2^T g_t)(t_0, x_{1,0}, x_{2,0}). \tag{3.4}$$

Hence, besides the given constraints (3.1b), a solution of (3.1) must satisfy the hidden constraints (3.4). Consequently, studying the solvability of the DAE (3.1), we must know all the hidden constraints and their solution properties. Solving the DAE (3.1) numerically, the hidden constraint (3.4) will not be satisfied in general as it is given implicitly only.
Hence, to ensure the existence of a unique solution and its accurate numerical approximation, we need all constraints explicitly given. For large DAEs obtained by automatic modeling software like Modelica or Dymola, however, the coupling of the algebraic and differential equations usually is hidden deep in the system and the constraints are given only implicitly. The difficulty to entangle this coupling and to filter out the constraints is measured by the *index* of the DAE. There are several index concepts, like the strangeness index [35, 36, 37, 38], the differentiation index [8, 9, 10, 11, 12, 13, 14], the tractability index [41, 42, 43, 44, 56, 57], the perturbation index [5, 23, 25] or the structural index [49, 53]. Applying numerical solvers directly to such higher index problems typically lead to severe problems in the numerical solution such as order reduction, inconsistent initial values and non-unique solutions, cp. e.g., [52].
To determine the index of the Honigmann model and to decide if the DAEs (2.1) - (2.3) specify unique solutions that can be computed numerically in an accurate and efficient fashion, we study the models using the concept of derivative arrays and the strangeness-index, cp. [35, 36, 37, 38]. The strangeness-index allows to classify a large class of DAE initial value problems, linear and nonlinear, over- and underdetermined, with respect to the existence and uniqueness of solutions. For those problems, the strangeness framework provides the tools to filter out the constraints and to remodel the problem such that it can be solved numerically with the same accuracy as ODEs.

For the purpose of this work, it is sufficient to consider *strangeness-free* systems, i.e., DAEs

$$F(t, x, \dot{x}) = 0 \tag{3.5}$$

with $F \in C(\mathbb{D}, \mathbb{R}^n)$, where $\mathbb{D} = \mathcal{I} \times \Omega_x \times \Omega_{\dot{x}}$, that can be transformed to uniquely solvable semi-explicit systems using a transformation of variables, i.e., no differentiation is needed, cp. [38].

Definition 3.1. *Consider the DAE* (3.5). *If* $F \in C^1(\mathbb{D}, \mathbb{R}^n)$, *then* (3.5) *is called* strangeness-free *(s-free) if there exists* $d \leq n \in \mathbb{N}$, *such that*

(i) $\operatorname{rank}(F_{\dot{x}}(z)) = d$,

(ii) $\operatorname{rank}((U_2^T F_x)(z)) = n - d$, *where* $\operatorname{span}(U_2(z)) = \operatorname{corange}(F_{\dot{x}}(z))$

(iii) $\ker(F_{\dot{x}}(z)) \cap \ker((U_2^T F_x(z)) = \{0\}$

for every $z = (t, x, v) \in F^{-1}(\{0\}) = \{(t, x, v) \in \mathbb{D} \,|\, F(t, x, v) = 0\}$. *If, in addition,* $F \in C^1(\mathbb{D}, \mathbb{R}^n)$ *and* $\operatorname{rank}(([F_{\dot{x}}, F_x + \frac{d}{dt} F_{\dot{x}}])(z)) = n$ *on* $F^{-1}(\{0\})$, *then* (3.5) *is called* regular.

ODEs, purely algebraic equations and semi-explicit systems of the form $\dot{x}_1 = f(t, x_1, x_2)$, $0 = g(t, x_1, x_2)$ with g_{x_2} nonsingular, are s-free. On $\mathbb{D}$, we denote the set of functions that are s-free or s-free and regular by

$$C^k_{\text{sfree}}(\mathbb{D}, \mathbb{R}^n) := \left\{ F \in C^k(\mathbb{D}, \mathbb{R}^n) \,|\, \text{ F is s-free } \right\}, \tag{3.6}$$

$$C^k_{\text{sfree,reg}}(\mathbb{D}, \mathbb{R}^n) := \left\{ F \in C^k(\mathbb{D}, \mathbb{R}^n) \,|\, \text{ F is s-free and regular } \right\}, \tag{3.7}$$

where $C^k(\mathbb{D}, \mathbb{R}^n)$ denotes the k-times continuous differentiable functions on $\mathbb{D}$. The set

$$\mathcal{L}_F := F^{-1}(\{0\}) \tag{3.8}$$

contains the *consistent initializations* of (3.5), while the set

$$\mathcal{C}_F := \{(t_0, x_0) \in \mathcal{I} \times \Omega_x \,|\, \exists v_0 \in \Omega_{\dot{x}} \colon (t_0, x_0, v_0) \in F^{-1}(\{0\})\} \tag{3.9}$$

contains the *consistent initial values.*
For a s-free system and a given solution with a consistent initial value, we can ensure the uniqueness of this solution [38]. If the system is regular and s-free, then we can also ensure the existence of a unique solution for every consistent initial value [38].

Theorem 3.1. *Consider the initial value problem*

$$F(t, x, \dot{x}) = 0, \quad x(t_0) = x_0. \tag{3.10}$$

1. *If* $F \in C^k_{sfree}(\mathbb{D}, \mathbb{R}^n)$ *and* $(t_0, x_0) \in \mathcal{C}_F$ *is solvable, then the solution is unique.*

2. *If* $F \in C^k_{sfree,reg}(\mathbb{D}, \mathbb{R}^n)$, *then* (3.10) *is uniquely solvable for every* $(t_0, x_0) \in \mathcal{C}_F$.

Integrating (3.10) numerically, Theorem 3.1 implies that s-free systems can be solved numerically with the same order of accuracy as for ODEs, see [38, p. 251].
If (3.5) is *not* s-free, then derivatives of (3.5) may have to be included to solve the system, if it is solvable at all. Applying a numerical solver directly to such a *higher index system*, the hidden constraints, redundant or inconsistent equations may lead to arbitrarily wrong numerical solution that violate the constraints, cp. e.g. [39].

3.1 The discharging step

For the discharging model (2.1), we find that the governing equations are strangeness-free and regular.

Lemma 3.1. *Consider the discharging model* (2.1). *If* $m_{flow} > 0$ *and* $h_{v,w} > h_{v,sol,isen}$, *then* (2.1) *is strangeness-free and regular.*

Proof. We check the assertions of Definition 3.1. Permuting (2.1) in a suitable way, the Jacobians with respect to $\dot{x}$ and x are given by

$$F_{dch,\dot{x}} = \begin{bmatrix} I_5 & \\ & 0_{16}, \end{bmatrix}, \quad F_{dch,x} = \begin{bmatrix} 0 & A_{12} & A_{13} & 0 \\ 0 & A_{22} & A_{23} & A_{24} \\ 0 & 0 & A_{33} & A_{34} \\ A_{41} & 0 & 0 & A_{44} \end{bmatrix}, \tag{3.11}$$

respectively, where the blocks in $F_{dch,x}$ are given by

$$A_{12} = \begin{bmatrix} -1 & 0 & 0 & 0 \\ 0 & 0 & 0 & 0 \\ -1 & 0 & 0 & 0 \\ 0 & 0 & 0 & 0 \\ 1 & 0 & 0 & 0 \end{bmatrix}, \qquad A_{13} = \begin{bmatrix} 0 & 0 & 0 & 0 & 0 & 0 & 0 \\ 1 & 0 & 0 & 0 & 0 & 0 & 0 \\ h_{v,w} & 0 & 0 & 0 & 0 & m_{flow} & 0 \\ -1 & 0 & 0 & 0 & 0 & 0 & 0 \\ -h_{v,sol} & m_{flow} & 0 & 0 & 0 & 0 & 0 \end{bmatrix},$$

$$A_{22} = \begin{bmatrix} \text{-}1 & 0 & 0 & 0 \\ 0 & 1 & 0 & 0 \\ 0 & 0 & \text{-}1 & 0 \\ 0 & 0 & 0 & 1 \end{bmatrix}, \qquad A_{23} = \begin{bmatrix} 0 & 0 & 0 & 0 & 0 & 0 & 0 \\ 0 & 1 & 0 & 0 & 0 & 0 & 0 \\ h_{v,w}\text{-}h_{v,sol} & \text{-}m_{flow} & 0 & 0 & 0 & m_{flow} & 0 \\ 0 & \text{-}f_{6,h_{v,sol}} & 0 & 0 & \text{-}f_{6,p_{sol}} & 0 & 0 \end{bmatrix},$$

$$A_{24} = \begin{bmatrix} G & \text{-}G & 0 & 0 & 0 \\ 0 & \text{-}1 & 0 & 0 & 0 \\ 0 & 0 & 0 & 0 & 0 \\ 0 & 0 & 0 & 0 & 0 \end{bmatrix}, \qquad A_{34} = \begin{bmatrix} 0 & 0 & 0 & 0 & 0 \\ 0 & 0 & 0 & 0 & 0 \\ 0 & 0 & 0 & 0 & 0 \\ 0 & 0 & 0 & 0 & 0 \\ \text{-}f_{7,T_{sol}} & 0 & 0 & 0 & \text{-}f_{7,X_{salt}} \\ 0 & \text{-}f_{3,T_w} & 0 & 0 & 0 \\ 0 & \text{-}f_{1,T_w} & 0 & 0 & 0 \end{bmatrix},$$

$$A_{33} = \begin{bmatrix} \frac{2m_{flow}}{K} & 0 & 0 & 0 & 2p_{sol} & 0 & \text{-}2p_w \\ 0 & \text{-}\frac{1}{h_{v,w}\text{-}h_{v,sol,isen}} & \frac{h_{v,w}\text{-}h_{v,sol}}{\left(h_{v,w}\text{-}h_{v,sol,isen}\right)^2} & 0 & 0 & \frac{h_{v,sol}\text{-}h_{v,sol,isen}}{\left(h_{v,w}\text{-}h_{v,sol,isen}\right)^2} & 0 \\ 0 & 0 & 1 & \text{-}f_{5,s_v} & \text{-}f_{5,p_{sol}} & 0 & 0 \\ 0 & 0 & 0 & 1 & 0 & \text{-}f_{4,h_{v,w}} & \text{-}f_{4,p_w} \\ 0 & 0 & 0 & 0 & 1 & 0 & 0 \\ 0 & 0 & 0 & 0 & 0 & 1 & 0 \\ 0 & 0 & 0 & 0 & 0 & 0 & 1 \end{bmatrix},$$

$$A_{41} = \begin{bmatrix} 0 & 0 & 0 & 0 & 0 \\ 0 & 0 & 0 & 0 & 0 \\ 0 & -h_w & 1 & 0 & 0 \\ 0 & 0 & 0 & -h_{sol} & 1 \\ 0 & 0 & 0 & \frac{m_{salt}}{m_{sol}^2} & 0 \end{bmatrix}, \quad A_{44} = \begin{bmatrix} \text{-}f_{8,T_{sol}} & 0 & 0 & 1 & \text{-}f_{8,X_{salt}} \\ 0 & \text{-}f_{2,T_w} & 1 & 0 & 0 \\ 0 & 0 & \text{-}m_w & 0 & 0 \\ 0 & 0 & 0 & \text{-}m_{sol} & 0 \\ 0 & 0 & 0 & 0 & 1 \end{bmatrix}.$$

Hence, $\operatorname{rank}(F_{dch,\dot{x}}(t,x,v)) = 5$ on $\mathbb{D}_{dch}$. Choosing $U_2 = [e_6, ..., e_{21}]$, where $e_1, ..., e_n$ denotes the standard canonical basis in $\mathbb{R}^n$, we have that $\operatorname{range}(U_2) = \operatorname{corange}(F_{dch,\dot{x}}(t,x,v))$ on $\mathbb{D}_{dch}$. To prove that $\operatorname{rank}(U_2^T F_{dch,x}(t,x,v)) = 16$ on $\mathbb{D}_{dch}$, we consider the diagonal blocks A_{22}, A_{33}, A_{44}. First, we find that $\operatorname{rank}(A_{22}(t,x,v)) = 4$ on $\mathbb{D}_{dch}$. For A_{33}, we have that $\operatorname{rank}(A_{33}) = 7$ on $\mathbb{D}_{dch}$ if and only if $m_{flow}, (h_{v,w} - h_{v,sol,isen}) > 0$. These relations are satisfied as long as there is a pressure drop between the working and the solution tank. For A_{44}, we have that $\operatorname{rank}(A_{44}(t,x,v)) = 5$ on $\mathbb{D}_{dch}$ as the partial derivatives $f_{8,T_{sol}}, f_{2,T_w}$ of the specific enthalpies are positive as the the specific enthalpies are strictly monotonic increasing [50] and the masses m_w, m_{sol} are strictly positive as the system is closed. Hence, $\operatorname{rank}(U_2^T F_{dch,x}(t,x,v)) = 16$ on $\mathbb{D}_{dch}$ if and only if $m_{flow}, h_{v,w} - h_{v,sol,isen} > 0$. In this case, $\operatorname{range}(T_1) = \ker(U_2^T F_{dch,x}(t,x,v))$ on $\mathbb{D}_{dch}$, where $T_1 = [e_1, ..., e_5]$. Choosing $T_2 = [e_6, ..., e_{21}]$, then $\operatorname{range}(T_2) = \ker(F_{dch,\dot{x}}(t,x,v))$ on $\mathbb{D}_{dch}$. Since $[T_1, T_2]$ is nonsingular, this implies that $\ker(F_{dch,\dot{x}}(z)) \cap \ker((U_2^T F_{dch,x}(z)) = \{0\}$ on $\mathbb{D}_{dch}$. Thus, the system (2.1) is strangeness-free.
To check the regularity condition, we note that $\frac{d}{dt} F_{\dot{x},dch} = 0$, such that it remains to prove that $\operatorname{rank}[F_{\dot{x},dch}, F_{x,dch}] = n$ on $\mathbb{D}_{dch}$. Since $\operatorname{corange}(F_{\dot{x},dh}) = \operatorname{range}(T_1)$ and $\operatorname{corange}(U_2^T F_{x,dh}) = \operatorname{range}(T_2)$, we have that $\operatorname{corange}(F_{dch,\dot{x}}(z)) \cap \operatorname{corange}((U_2^T F_{dch,x}(z)) = \{0\}$ on $\mathbb{D}_{dch}$. Hence, $\operatorname{rank}[F_{\dot{x},dch}, F_{x,dch}] = n$ on $\mathbb{D}_{dch}$. □

The pressure drop from the working fluid tank to the solution tank induces a positive mass flow between these tanks. The energy balance at the turbine requires the specific enthalpy at the inlet of the turbine $h_{v,w}$ to be larger than the specific enthalpy at the outlet of the turbine $h_{v,sol}$ for every $t \in \mathcal{I}$ and we have that $h_{v,sol,isen} < h_{v,sol}$ for $\eta_{isen} = 0.92 < 1$, cp. [64, fig. 5.10, p. 44]. Hence, as long as the pressure difference between the two tanks is non-zero, i.e., $p_w > p_{sol}$, the mathematical model (2.1) is s-free and regular. Denoting the set of consistent initializations for which $p_w > p_{sol}$ by

$$\mathcal{L}_{dch} := \{(t_0, x_0, v_0) \in \mathcal{L}_{dh} \| , p_{w,0} > p_{sol,0}\} \tag{3.12}$$

and the associated consistent initial values by

$$\hat{\mathcal{C}}_{dch} := \{(t_0, x_0) \in \mathcal{L}_{dch}\}, \tag{3.13}$$

then Theorem 3.1 ensures that for every $(t_0, x_0) \in \hat{\mathcal{C}}_{dch}$, there exists a unique solution describing the evolution of the discharging from this initial value.
This solution exists until the pressure is balanced and the system has reached its equilibrium. At this point, the mass flow vanishes and the block matrix A_{33} becomes singular. Then, the DAE model (2.1) changes its s-index and solutions cease to exist.
For a consistent, admissible initial value $(t_0, x_0) \in \hat{\mathcal{C}}_{dch}$, the solution can be computed numerically with the same order of accuracy as for ODEs. Together with the physical verification of the model in [64], we thus find that the discharge model is a physically meaningful model for the discharging and allows to simulate the discharge with a measurable accuracy. However, due to the different scales in the model, the equations still pose some difficulties on the numerical solvers. We illustrate these issues in Section 5.

3.2 The charging step

We first study the model for the main desorption step, then we turn to the models of the transition phases.

3.2.1 The desorption step

The model equations (2.2) of the desorption step are not strangeness-free.

Lemma 3.2. *The charge model* (2.2) *is neither regular nor strangeness-free.*

Proof. Again, we check the assertions of Definition 3.1. For system (2.2), the Jacobians with respect to $\dot{x}$ and x are given by

$$F_{ch,\dot{x}} = \begin{bmatrix} I_6 & \\ & 0_{14}, \end{bmatrix}, \quad F_{ch,x} = \begin{bmatrix} 0 & A_{12} & A_{13} \\ 0 & A_{22} & A_{23} \\ A_{31} & A_{32} & A_{33} \end{bmatrix}, \tag{3.14}$$

where the blocks in $F_{ch,x}$ are given by

$$A_{12} = \begin{bmatrix} -1 & 0 & 0 & 0 & 0 & 0 & 0 \\ 0 & -1 & 0 & 0 & 0 & 0 & 0 \\ 0 & 0 & 0 & 0 & 0 & 0 & 0 \\ -1 & 0 & 0 & 0 & 0 & 0 & 0 \\ 0 & 0 & 0 & 0 & 0 & 0 & 0 \\ 0 & 1 & 0 & 0 & 0 & 0 & 0 \end{bmatrix}, \quad A_{13} = \begin{bmatrix} 0 & 0 & 0 & 0 & 0 & 0 & 0 \\ 0 & 0 & 0 & 0 & 0 & 0 & 0 \\ 0 & 0 & 0 & 0 & 0 & 0 & 1 \\ 0 & 0 & 0 & m_{flow} & 0 & 0 & h_{v,w} \\ 0 & 0 & 0 & 0 & 0 & 0 & -1 \\ 0 & 0 & 0 & 0 & -m_{flow} & 0 & -h_{v,sol} \end{bmatrix},$$

$$A_{22} = \begin{bmatrix} -1 & 0 & G_w & 0 & 0 & 0 & 0 \\ 0 & -1 & 0 & G_{sol} & 0 & 0 & 0 \\ 0 & 0 & 0 & -1 & 0 & 1 & 0 \\ 0 & 0 & 0 & 0 & 1 & 0 & -f_{6,p_w} \\ 0 & 0 & 0 & 0 & 0 & 0 & 1 \\ 0 & 0 & 0 & 0 & 0 & 0 & 0 \\ 0 & 0 & 0 & -f_{7,T_{sol}} & 0 & 0 & 0 \end{bmatrix}, \quad A_{23} = \begin{bmatrix} 0 & 0 & 0 & 0 & 0 & 0 & 0 \\ 0 & 0 & 0 & 0 & 0 & 0 & 0 \\ 0 & 0 & 0 & 0 & 0 & 0 & 0 \\ 0 & 0 & 0 & -f_{6,h_{v,w}} & 0 & 0 & 0 \\ -1 & 0 & 0 & 0 & 0 & 0 & 0 \\ 0 & 0 & 0 & 1 & -1 & 0 & 0 \\ 1 & 0 & 0 & 0 & 0 & -f_{7,X_{salt}} & 0 \end{bmatrix},$$

$$A_{31} = \begin{bmatrix} 0 & 0 & 0 & 0 & 0 & 0 \\ 0 & 0 & 0 & 0 & 0 & 0 \\ 0 & 0 & 0 & 0 & 0 & 0 \\ 0 & 0 & 0 & 0 & 0 & 0 \\ 1 & 0 & -h_w & 0 & 0 & 0 \\ 0 & 1 & 0 & -h_{sol} & 0 & 0 \\ 0 & 0 & 0 & \frac{m_{salt}}{m_{sol}^2} & 0 & 0 \end{bmatrix}, \quad A_{32} = \begin{bmatrix} 0 & 0 & 0 & -f_{3,T_{sol}} & 0 & 0 & 0 \\ 0 & 0 & -f_{1,T_w} & 0 & 0 & 0 & 1 \\ 0 & 0 & 0 & -f_{8,T_{sol}} & 0 & 0 & 0 \\ 0 & 0 & -f_{2,T_w} & 0 & 0 & 0 & 0 \\ 0 & 0 & 0 & 0 & 0 & 0 & 0 \\ 0 & 0 & 0 & 0 & 0 & 0 & 0 \\ 0 & 0 & 0 & 0 & 0 & 0 & 0 \end{bmatrix},$$

$$A_{33} = \begin{bmatrix} 0 & 0 & 0 & 0 & 1 & 0 & 0 \\ 0 & 0 & 0 & 0 & 0 & 0 & 0 \\ 0 & 0 & 1 & 0 & 0 & -f_{8,X_{salt}} & 0 \\ 0 & 1 & 0 & 0 & 0 & 0 & 0 \\ 0 & -m_w & 0 & 0 & 0 & 0 & 0 \\ 0 & 0 & -m_{sol} & 0 & 0 & 0 & 0 \\ 0 & 0 & 0 & 0 & 0 & 1 & 0 \end{bmatrix}.$$

Hence, $\operatorname{rank}(F_{ch,\dot{x}}(t,x,v)) = 6$ on $\mathbb{D}_{ch}$. Choosing $Z_2 = [e_7, ..., e_{21}]$, we have that $\ker(F_{ch,\dot{x}}(t,x,v)) = \operatorname{span}(Z_2)$ on $\mathbb{D}_{ch}$.
Due to the common zero column of A_{23}, A_{33}, however, $\operatorname{rank}(U_2^T F_{ch,x}(t,x,v)) < 14$ on $\mathbb{D}_{ch}$, implying that (2.2) is not s-free. □

The model (2.2) of the desorption step in the charging process as derived is neither regular nor strangeness-free as it lacks an equation specifying the mass flow between the tanks. In the discharging model (2.1), the mass flow through the turbine was modeled by the Stodola equation (2.1p). In the desorption step, however, there is no equation specifying the mass flow through the open valve and, consequently, the desorption model (2.2) is not s-free. Hence, using (2.2) as a model of the absorption step, we cannot ensure the existence or uniqueness of a solution for a consistent initial value. Consequently, the numerical solution may be arbitrarily wrong and violate the constraints.
To find a properly stated, strangeness-free model, we can either use the strangeness framework for higher index systems, cp. [38], or we can remodel the system physically by adding an appropriate equation for the mass flow rate. Using derivative arrays and the strangeness index, we may be able to remodel the equations (2.2) such that they yield a strangeness-free and regular model for the desorption step. Taking a closer look to the equations (2.2), however, we find that (4.9k), (4.9o) and (4.9m) only determine p_w and p_{sol} as T_w, T_{sol} and X_{Salt} are given by the initial conditions, cp. Section 4.1. Hence, one of the equations (4.9k), (4.9o) and (4.9m) is redundant. Replacing this redundant equation by one containing the mass flow rate m_{flow}, the model may be turned into a strangeness-free system. One way to obtain such a relation could be the insertion of a pipe with a vapor flow between the tanks. As such a pipe imposes a small pressure drop between the two tanks, it can be used to obtain one equation for the mass flow rate m_{flow}.

3.2.2 The intermediate steps

For the intermediate steps in the charging process, the model equations (2.3) are strangeness-free and regular.

Lemma 3.3. *The charge model* (2.3) *is regular and strangeness-free.*

Proof. Permuting (2.3) in a suitable way, the Jacobians with respect to $\dot{x}$ and x are given by

$$F_{int,\dot{x}} = \begin{bmatrix} I_6 & \\ & 0_{14}, \end{bmatrix}, \quad F_{int,x} = \begin{bmatrix} 0 & A_{12} & A_{13} \\ 0 & A_{22} & A_{23} \\ 0 & 0 & A_{23} \end{bmatrix}, \tag{3.15}$$

where the blocks A_{12} and A_{13} in $F_{int,x}$ coincide with the same-named blocks in $F_{ch,x}$. The block A_{33} in $F_{int,x}$ coincides with the block A_{44} in $F_{dch,x}$ and is therefore regular[1]. The remaining blocks A_{22} and A_{23} are given by

$$A_{22} = \begin{bmatrix} -1 & 0 & 0 & 0 & 0 & 0 & 0 & 0 & 0 \\ 0 & -1 & 0 & 0 & 0 & 0 & 0 & 0 & 0 \\ 0 & 0 & 1 & 0 & 0 & 0 & 0 & 0 & 0 \\ 0 & 0 & 0 & 1 & 0 & 0 & 0 & 0 & 0 \\ 0 & 0 & 0 & 0 & 1 & 0 & 0 & 0 & -f_{3,T_{v,w}} \\ 0 & 0 & 0 & 0 & 0 & 1 & 0 & 0 & 0 \\ 0 & 0 & 0 & 0 & 0 & 0 & 1 & 0 & 0 \\ 0 & 0 & 0 & 0 & 0 & 0 & 0 & 1 & 0 \\ 0 & 0 & 0 & 0 & 0 & 0 & 0 & 0 & 1 \end{bmatrix}, \quad A_{23} = \begin{bmatrix} 0 & G_w & 0 & 0 & 0 \\ G_{sol} & 0 & 0 & 0 & 0 \\ 0 & 0 & 0 & 0 & 0 \\ -f_{7,T_{sol}} & 0 & 0 & 0 & -f_{7,X_{salt}} \\ 0 & 0 & 0 & 0 & 0 \\ -1 & 0 & 0 & 0 & 0 \\ 0 & -f_{1,T_w} & 0 & 0 & 0 \\ -f_{3,T_{sol}} & 0 & 0 & 0 & 0 \\ 0 & -1 & 0 & 0 & 0 \end{bmatrix}.$$

[1] The reason for the identity needs to be investigated in more detail.

Hence, $\operatorname{rank}(F_{int,\dot{x}}(t,x,v)) = 6$ on $\mathbb{D}_{int}$. Choosing $Z_2 = [e_7, ..., e_{21}]$, then $\ker(F_{int,\dot{x}}(t,x,v)) = \operatorname{span}(Z_2)$ on $\mathbb{D}_{int}$.

□

4 Remodeling of the Honigmann process

To study system immanent properties like positivity and to allow for a numerical solution using standard MATLAB solvers, we reformulate (2.1) as a semi-explicit system.

Lemma 4.1. *Consider the discharge model* (2.1) *and let* $(t_0, x_0) \in \hat{\mathcal{C}}_{dch}$. *A function* x *solves* (2.1) *with initial condition* $x(t_0) = x_0$ *if and only if* x *solves the semi-explicit system*

$$\dot{H}_w = m_{flow}(m_w, H_w, m_{sol}, H_{sol})\ h_{v,w}(m_w, H_w) + Q_{flow}, \tag{4.1a}$$
$$\dot{H}_{sol} = m_{flow}(m_w, H_w, m_{sol}, H_{sol})\ h_{v,sol,isen}(m_w, H_w) - Q_{flow}, \tag{4.1b}$$
$$\dot{m}_w = -m_{flow}(m_w, H_w, m_{sol}, H_{sol}), \tag{4.1c}$$
$$\dot{m}_{sol} = m_{flow}(m_w, H_w, m_{sol}, H_{sol}), \tag{4.1d}$$
$$\dot{Q} = Q_{flow} \tag{4.1e}$$

and

$$Q_{flow} = G \cdot \left(f_{8,1}^{-1}(\tfrac{H_{sol}}{m_{sol}}, \tfrac{m_{salt}}{m_{sol}}) - f_2^{-1}(\tfrac{H_w}{m_w}) \right), \tag{4.2a}$$
$$T_{vap,w} = f_2^{-1}(\tfrac{H_w}{m_w}), \tag{4.2b}$$
$$P_m = \sqrt{K(p_w^2 - p_{sol}^2)} \cdot \left(f_3\big(f_2^{-1}(\tfrac{H_w}{m_w})\big) - h_{v,sol} \right), \tag{4.2c}$$
$$T_{v,sol} = f_6\left(f_5\left(s_v, p_{sol}\right), p_{sol}\right), \tag{4.2d}$$
$$m_{flow} = \sqrt{K(f_1^2\big(f_2^{-1}(\tfrac{H_w}{m_w})\big) - f_7^2\big(f_{8,1}^{-1}(\tfrac{m_{salt}}{m_{sol}}, \tfrac{H_{sol}}{m_{sol}}), \tfrac{H_{sol}}{m_{sol}}\big))}, \tag{4.2e}$$
$$h_{v,sol} = f_3\big(f_2^{-1}(\tfrac{H_w}{m_w})\big) - \eta_{isen}\Big(f_3\big(f_2^{-1}(\tfrac{H_w}{m_w})\big) - h_{v,sol,isen}\Big), \tag{4.2f}$$
$$h_{v,sol,isen} = f_5\left(s_v, p_{sol}\right), \tag{4.2g}$$
$$s_v = f_4\left(f_3\big(f_2^{-1}(\tfrac{H_w}{m_w})\big), f_1\big(f_2^{-1}(\tfrac{H_w}{m_w})\big)\right), \tag{4.2h}$$
$$p_{sol} = f_7\big(f_{8,1}^{-1}(\tfrac{H_{sol}}{m_{sol}}, \tfrac{m_{salt}}{m_{sol}}), \tfrac{m_{salt}}{m_{sol}}\big), \tag{4.2i}$$
$$h_{v,w} = f_3\big(f_2^{-1}(\tfrac{H_w}{m_w})\big), \tag{4.2j}$$
$$p_w = f_1\big(f_2^{-1}(\tfrac{H_w}{m_w})\big), \tag{4.2k}$$
$$T_{sol} = f_{8,1}^{-1}(\tfrac{H_{sol}}{m_{sol}}, \tfrac{m_{salt}}{m_{sol}}), \tag{4.2l}$$
$$T_w = f_2^{-1}(\tfrac{H_w}{m_w}), \tag{4.2m}$$
$$h_w = \frac{H_w}{m_w}, \tag{4.2n}$$
$$h_{sol} = \frac{H_{sol}}{m_{sol}}, \tag{4.2o}$$
$$X_{salt} = \frac{m_{salt}}{m_{sol}}, \tag{4.2p}$$

with initial condition $[I_5, 0]x_0 = [H_{w,0}, H_{sol,0}, m_{w,0}, m_{sol,0}, Q_0]$.

Proof. If $(t_0, x_0) \in \hat{\mathcal{C}}_{dch}$, then the DAE (2.1) with initial condition $x(t_0) = x_0$ is s-free and regular and the Jacobian $F_{dch,x_2}(t_0, x_0)$ is nonsingular, where $x_2 = [0, I_{16}]x$ denotes the components occurring without derivatives. By the Implicit Function Theorem, the algebraic equations $[0, I_{16}]F_{dch}$ can be uniquely solved for x_2, leading to the equations (4.2). Solving the differential equations $[I_5, 0]F_{dch}$ for $x_1 = [I_5, 0]x$ and inserting (4.2) for x_2, then we obtain equations (4.1). □

Setting

$$x_d = \left[x_1^T, 0\right]^T, \quad x_a = \left[0, x_2^T\right]^T$$

and

$$h_{MP} = \left[h^T, 0\right]^T, \quad g_{MP} = \left[0, g^T\right]^T, \tag{4.3}$$

the system

$$\dot{x}_d = h_{MP}(t, x_d), \quad x_a = g_{MP}(t, x_a)$$

correponds to the *Moore-Penrose remodeling* of the discharge model [3]. The Moore-Penrose remodeling filters out the differential and algebraic components in a s-free DAE $F(t, x, \dot{x}) = 0$ using the Moore-Penrose projection F^+F [3].
In Section 5, we use the explicit reformulation (4.1), (4.2) to simulate the discharging step using standard MATLAB solvers.

The Moore-Penrose remodeling allows to study the positivity of a DAE, i.e., to determine whether a given solution remains componentwise nonnegative if the initial value was componentwise nonnegative. For the Honigmann process, in which the considered variables describe real quantities that cannot take negative values, the property of positivity is a key ingredient to obtain a realistic model.
We denote the set of consistent, admissible and nonnegative initial values by $\hat{\mathcal{C}}_{dch}^+ := \hat{\mathcal{C}}_{dch} \cap \mathbb{R} \times \mathbb{R}_+^n$.

Lemma 4.2. *Consider the discharge model* (2.1). *For every* $(t_0, x_0) \in \hat{\mathcal{C}}_{dch}^+$ *, the initial value problem* (2.1) *with* $x(t_0) = x_0$ *is positive.*

Proof. With $F_{dch,\dot{x}} = \left[\begin{smallmatrix} I_5 & 0_{16,} \end{smallmatrix}\right]$, cp. (3.11), the Moore-Penrose projection $P_{MP} = F_{dch,\dot{x}}^+ F_{dch,\dot{x}}$ is given by $P_{MP} = \left[\begin{smallmatrix} I_5 & 0_{16,} \end{smallmatrix}\right]$, leading to the special structure of h_{MP}, g_{MP} as in (4.3). Noting that the discharge model is positive if and only if there exists a function $\kappa \colon \hat{\mathcal{C}}_{dch}^+ \to \mathbb{R}_+$, such that

$$\hat{\kappa}\, x_{d,0} + h_{MP,0}\big(t_0, x_{d,0}\big) \geq -\hat{\kappa}\, g_{MP,0}\big(t_0, x_{d,0}\big) - \dot{g}_{MP,0}\big(t_0, x_{d,0}\big) \tag{4.4}$$

on $\hat{\mathcal{C}}_{dch}^+$ and for every $\hat{\kappa} \geq \kappa(t_0, x_0)$, cp. [4, Cor. 5.3.1]. Due to the special structure, this implies that (4.4) is satisfied if and only if

$$h(t_0, x_{1,0}) \geq -\hat{\kappa}\, x_{1,0}, \tag{4.5}$$

$$\hat{\kappa}\, g(t_0, x_{1,0}) \geq -\dot{g}(t_0, x_{1,0}) \tag{4.6}$$

on $\hat{\mathcal{C}}_{dch}^+$ and for every $\hat{\kappa} \geq \kappa(t_0, x_0)$. As the material functions $f_1, ..., f_6, f_8$ as well as the specific enthalpies and masses are strictly positive on the set $\hat{\mathcal{C}}_{dch}$, we have that $g_{MP} > 0$ on $\hat{\mathcal{C}}_{dch}$. Furthermore, as the differential components $x_d > 0$ for $x \in \hat{\mathcal{C}}_{dch}$, there exists a function $\kappa \colon \hat{\mathcal{C}}_{dch}^+ \to \mathbb{R}_+$ satisfying (4.5) and (4.6). Hence, the system (2.1) is positive. □

Hence, the mathematical model (2.1) reflects the physical property of positivity.

4.1 Initial conditions

Exploiting the semi-explicit reformulation (4.1), (4.2) of the discharge model, consistent initial values can easily be chosen by prescribing initial conditions for the differential variables $x_1 = [I_5, 0]x$ and computing the remaining initial values for the algebraic variables $x_2 = [0, I-16]x$ using (4.2). However, as the differential components involve quantities like the enthalpies H_w, H_{sol} that cannot be directly measured, this 'mathematical' approach has to be discarded and directly influenceable and measurable quantities like pressure, temperature, mass and concentration are chosen as design variables. Denoting these components by $\tilde{x}_1$ and the remaining components by $\tilde{x}_2$, such that $\Pi^T x = [\tilde{x}_1^T, \tilde{x}_2^T]^T$ for a permutation $\Pi \in \mathbb{R}^{21\times 21}$, the remaining initial values are computed by solving the algebraic equations $[0, I_{16}]F_{dch} = 0$ for $\tilde{x}_2$. As the system $F_{dch}(t, x, \dot{x}) = 0$ is strangeness-free, the Jacobian $F_{dch,\tilde{x}_2}$ has full row rank and $[0, I_{16}]F_{dch} = 0$ is uniquely solvable for $\tilde{x}_{2,0}$.
To initialize the discharging procedure in $t_0 = 0$, we choose the masses $m_{w,0}$, $m_{sol,0}$ and the temperatures $T_{w,0}$, $T_{sol,0}$ of the water and the solution, respectively, as well as the salt concentration $X_{salt,0} = m_{salt}/m_{sol,0}$ as design variables, i.e., we set

$$\tilde{x}_1 := [m_{w,0}, m_{sol,0}, T_{w,0}, T_{sol,0}, X_{salt,0}]^T.$$

As the Lithium Bromide concentration in the solution is known at the beginning, and since we assume that only water without salt (LiBr) is evaporating, the salt mass can be calculated from the initial salt concentration and the initial mass of the solution and remains constant for all $t \in \mathcal{I}$, cp. (4.7g). For the initial temperatures, we assume a difference of 10 K, reflecting the heat transfer between the tanks which is realized by a water circuit.
Summarizing the remaining components of x in $\tilde{x}_2$ and solving (2.1) for $\tilde{x}_2$, we obtain the initial

value

$$
\begin{aligned}
Q_0 &= 0, && (4.7a)\\
m_{w,0} &= 2, && (4.7b)\\
m_{sol,0} &= 3, && (4.7c)\\
T_{sol,0} &= 120 + 273.15, && (4.7d)\\
T_{w,0} &= 110 + 273.15, && (4.7e)\\
X_{salt,0} &= 0.65, && (4.7f)\\
m_{salt} &= m_{sol,0} X_{salt,0}, && (4.7g)\\
Q_{flow,0} &= G\left(T_{sol,0} - T_{w,0}\right), && (4.7h)\\
p_{w,0} &= f_1(T_{w,0}), && (4.7i)\\
h_{w,0} &= f_2(T_{w,0}), && (4.7j)\\
H_{w,0} &= m_{w,0} h_{w,0}, && (4.7k)\\
T_{v,w,0} &= T_{w,0}, && (4.7l)\\
h_{v,w,0} &= f_3(T_{w,0}), && (4.7m)\\
s_{v,0} &= f_4(h_{v,w,0}, p_{w,0}), && (4.7n)\\
p_{sol,0} &= f_7(T_{sol,0}, X_{Salt,0}), && (4.7o)\\
h_{sol,0} &= f_8(T_{sol,0}, X_{Salt,0}), && (4.7p)\\
H_{sol,0} &= m_{sol,0} h_{sol,0}, && (4.7q)\\
h_{v,sol,isen,0} &= f_5(s_{v,0}, p_{sol,0}), && (4.7r)\\
h_{v,sol,0} &= h_{v,w,0} - eta_{isen}\left(h_{v,w,0} - h_{v,sol,isen,0}\right), && (4.7s)\\
T_{v,sol,0} &= f_6(h_{v,sol,0}, p_{sol,0}), && (4.7t)\\
m_{flow,0} &= \sqrt{\left(K\left(p_{w,0}^2 - p_{sol,0}^2\right)\right)}, && (4.7u)\\
P_{m,0} &= m_{flow,0}\left(h_{v,w,0} - h_{v,sol,0}\right). && (4.7v)
\end{aligned}
$$

To solve (2.1) numerically with a Runge-Kutta method, we further need an initial condition for the gradient $\dot{x}_0$. Given x_0, then $\dot{x}_0$ can be computed using the semi-explicit reformulation (4.2) and (4.1). More precisely, we have that $\dot{x}_{1,0} = h(t_0, x_{1,0})$, for $\dot{x}_{2,0}$ we consider finite differences and use that $\dot{x}_{2,0} = (g(t_0 + \tau, x_{1,0} + \tau\dot{x}_{1,0}) - g(t_0, x_{1,0}))/\tau + \mathcal{O}(\tau^2)$ for $\tau > 0$ sufficiently small.

Remark 4.1. *Studied in a cyclic process, the charging step is initialized with the final states of the discharging step. Assuming that the desorption process is isobaric, i.e. the pressure in both tanks is equal, the so-called charging step I is needed between discharge and the desorption (charging step II), cp. Section 2.2.4. In this step, the valve is closed and the tanks are brought to equal pressure by heat transfer. It is necessary for the modeling because the discharge does not exactly terminate at equal pressures. Nevertheless, numerically it is possible to use the final values of the discharging step for charging step II (cp. Section 2.2.3) in the reference case because step I is short enough to be neglected here. The analysis of the model equations* (4.9d) *to* (4.9t) *in Section 3.2.1 show that the system is not strangeness-free and need either a physical remodeling or an index reduction which will be subject of further research.*

4.2 Summary of model equations

Before we turn to the numerical simulation of the Honigmann process, we summarize the DAE models and list the physical units of the variables and functions.
For the discharging step, we obtain the system

$$
\begin{aligned}
0 &= \dot{Q} - Q_{flow}, && \text{(4.8a)}\\
0 &= \dot{m}_w + m_{flow}, && \text{(4.8b)}\\
0 &= \dot{H}_w + m_{flow} h_{v,w} - Q_{flow}, && \text{(4.8c)}\\
0 &= \dot{m}_{sol} - m_{flow}, && \text{(4.8d)}\\
0 &= \dot{H}_{sol} - m_{flow} h_{v,sol} + Q_{flow}, && \text{(4.8e)}\\
0 &= G \cdot (T_{sol} - T_w) - Q_{flow}, && \text{(4.8f)}\\
0 &= T_{v,w} - T_w, && \text{(4.8g)}\\
0 &= m_{flow} \cdot (h_{v,w} - h_{v,sol}) - P_m, && \text{(4.8h)}\\
0 &= T_{v,sol} - f_6\left(h_{v,sol}, p_{sol}\right), && \text{(4.8i)}\\
0 &= \frac{m_{flow}^2}{K} + p_{sol}^2 - p_w^2, && \text{(4.8j)}\\
0 &= \frac{h_{v,w} - h_{v,sol}}{h_{v,w} - h_{v,sol,isen}} - \eta_{isen}, && \text{(4.8k)}\\
0 &= h_{v,sol,isen} - f_5\left(s_v, p_{sol}\right), && \text{(4.8l)}\\
0 &= s_v - f_4\left(h_{v,w}, p_w\right), && \text{(4.8m)}\\
0 &= p_{sol} - f_7\left(T_{sol}, X_{salt}\right), && \text{(4.8n)}\\
0 &= h_{v,w} - f_3\left(T_w\right), && \text{(4.8o)}\\
0 &= p_w - f_1\left(T_w\right), && \text{(4.8p)}\\
0 &= h_{sol} - f_8\left(T_{sol}, X_{salt}\right), && \text{(4.8q)}\\
0 &= h_w - f_2\left(T_w\right), && \text{(4.8r)}\\
0 &= H_w - h_w m_w, && \text{(4.8s)}\\
0 &= H_{sol} - h_{sol} m_{sol}, && \text{(4.8t)}\\
0 &= X_{salt} - \frac{m_{salt}}{m_{sol}}. && \text{(4.8u)}
\end{aligned}
$$

and for the charging step, we obtain the system

$$
\begin{aligned}
0 &= \dot{Q}_w - Q_{flow,w}, && \text{(4.9a)}\\
0 &= \dot{Q}_{sol} - Q_{flow,sol}, && \text{(4.9b)}\\
0 &= \dot{m_w} + m_{flow}, && \text{(4.9c)}\\
0 &= \dot{H}_w + m_{flow} h_{v,w} - Q_{flow,w}, && \text{(4.9d)}\\
0 &= \dot{m}_{sol} - m_{flow}, && \text{(4.9e)}\\
0 &= \dot{H}_{sol} - m_{flow} h_{v,sol} + Q_{flow,sol}, && \text{(4.9f)}\\
0 &= G_w \cdot (T_w - T_{w,q}) - Q_{flow,w}, && \text{(4.9g)}\\
0 &= G_{sol} \cdot (T_{sol} - T_{sol,q}) - Q_{flow,sol}, && \text{(4.9h)}\\
0 &= T_{v,sol} - T_{sol}, && \text{(4.9i)}\\
0 &= T_{v,w} - f_6 \left(h_{v,w}, p_w\right), && \text{(4.9j)}\\
0 &= p_w - p_{sol}, && \text{(4.9k)}\\
0 &= h_{v,w} - h_{v,sol}, && \text{(4.9l)}\\
0 &= p_{sol} - f_7 \left(T_{sol}, X_{salt}\right), && \text{(4.9m)}\\
0 &= h_{v,sol} - f_3 \left(T_{sol}\right), && \text{(4.9n)}\\
0 &= p_w - f_1 \left(T_w\right), && \text{(4.9o)}\\
0 &= h_{sol} - f_8 \left(T_{sol}, X_{salt}\right), && \text{(4.9p)}\\
0 &= h_w - f_2 \left(T_w\right), && \text{(4.9q)}\\
0 &= H_w - h_w m_w, && \text{(4.9r)}\\
0 &= H_{sol} - h_{sol} m_{sol}, && \text{(4.9s)}\\
0 &= X_{salt} - \frac{m_{salt}}{m_{sol}}. && \text{(4.9t)}
\end{aligned}
$$

The parameters and functions used here are summarized in Table 1, the variables for the discharging step in 2 and for the charging step in Table 3.

Table 1: Explanation of parameters and functions (discharge and charge)

physical name	unit	physical description
Parameters		
G	$\frac{kW}{K}$	thermal conductance (G_w and G_{sol} for the charging step where each tank has a thermal port with a temperature source or sink, cp. figure 2.1)
K	$\frac{kg^2}{bar^2}$	constant from the Stodola equation for turbines in part load [34] (discharging step only)
η_{isen}	$-$	isentropic efficiency of the turbine (discharging step only)
m_{salt}	kg	mass of salt dissolved in the solution (can not evaporate)
$T_{w,q}$, $T_{sol,q}$	K	temperature of the temperature source/sink on the working fluid and solution side (charging step only)
Functions (at least C1 functions)		
$f_1(T_w)$	bar	$p_{eq,w}(T_w)$ - equilibrium pressure function of the working fluid for at least 273.15 K $\leq T_w \leq$ 1073.15 K, [30]
$f_2(T_w)$	$\frac{kJ}{kg}$	$h_{eq,w}(T_w)$ - specific enthalpy function of the working fluid for at least 273.15 K $\leq T_w \leq$ 1073.15 K, [30]
$f_3(T_w)$	$\frac{kJ}{kg}$	$h_{eq,vap}(T_w)$ - specific enthalpy function of the vapour (at the working fluid side) for at least 273.15 K $\leq T_w \leq$ 1073.15 K, [30]
$f_4(h_{v,w}, p_w)$	$\frac{kJ}{kg\,K}$	$s_v(h_{v,w}, p_w)$ - specific entropy function of the vapour for at least 273.15 K $\leq T_w \leq$ 1073.15 K and $p \leq$ 500 bar, [30]
$f_5(s_v, p_{sol})$	$\frac{kJ}{kg}$	$h_{eq,vap}(s_v, p_{sol})$ - specific enthalpy function of the vapour (isentropic, at the solution side) for at least 273.15 K $\leq T_w \leq$ 1073.15 K and $p \leq$ 500 bar, [30]
$f_6(h_{v,sol}, p_{sol})$	K	$T_v(h_{v,sol}, p_{sol})$ - temperature function of the vapour for at least 273.15 K $\leq T_v \leq$ 1073.15 K and $p \leq$ 500 bar, [30]
$f_7(T_{sol}, X_{salt})$	bar	$p_{eq,sol}(T_{sol}, X_{salt})$ - equilibrium pressure function of the solution for 273.15 K $\leq T_{sol} \leq$ 500 K and at least $0.4\frac{kg_{LiBr}}{kg_{solution}} < X_{salt} < 0.75\frac{kg_{LiBr}}{kg_{solution}}$, [50]
$f_8(T_{sol}, X_{salt})$	$\frac{kJ}{kg}$	$h_{eq,sol}(T_{sol}, X_{salt})$ - specific enthalpy of the solution at equilibrium for 273.15 K $\leq T_{sol} \leq$ 500 K and at least $0.4\frac{kg_{LiBr}}{kg_{solution}} < X_{salt} < 0.75\frac{kg_{LiBr}}{kg_{solution}}$, [50]

Table 2: Explanation of the variables (discharge)

physical variable name	unit	physical description
Q	kJ	heat transfered from the solution tank to the working fluid tank
m_w	kg	mass of water in the working fluid tank
H_w	kJ	enthalpy of the working fluid
m_{sol}	kg	mass of solution in the solution tank
H_{sol}	kJ	enthalpy of the solution
h_w	$\frac{kJ}{kg}$	specific enthalpy of the working fluid
Q_{flow}	kW	heat flow rate from the solution tank to the working fluid tank
m_{flow}	$\frac{kg}{s}$	mass flow rate between the two tanks
T_{sol}	K	temperature in the solution tank
$T_{v,w}$	K	temperature of the vapour on the working fluid side
$h_{v,w}$	$\frac{kJ}{kg}$	specific enthalpy of the vapour on the working fluid side
P_m	kW	mechanical work produced by the turbine
s_v	$\frac{J}{kg\,K}$	specific entropy of the vapour at the turbine entrance/ working fluid side
$h_{v,sol,isen}$	$\frac{kJ}{kg}$	specific enthalpy of the vapour at the turbine outlet in isentropic case
$h_{v,sol}$	$\frac{kJ}{kg}$	specific enthalpy of the vapour at the turbine outlet/ solution side
$T_{v,sol}$	K	temperature of the vapour at the turbine outlet/ solution side
p_{sol}	bar	pressure of the solution
h_{sol}	$\frac{kJ}{kg}$	specific enthalpy of the solution
T_w	K	temperature in the working fluid tank
X_{salt}	$\frac{kg\,salt}{kg\,sol}$	mass concentration of salt in the solution
p_w	bar	pressure in the working fluid tank

Table 3: Explanation of the variables (charge)

physical variable name	unit	physical description
Q_w	kJ	Heat transfered between the working fluid tank and the temperature source/sink
Q_{sol}	kJ	Heat transfered between the solution tank and the temperature source/sink
m_w	kg	mass of working fluid in the working fluid tank
H_w	kJ	enthalpy of the working fluid
m_{sol}	kg	mass of solution in the solution tank
H_{sol}	kJ	enthalpy of the solution
$Q_{flow,w}$	kW	heat flow rate between the working fluid tank and the temperature source/sink
$Q_{flow,sol}$	kW	heat flow rate between the solution tank and the temperature source/sink
T_w	K	temperature in the working fluid tank
T_{sol}	K	temperature in the solution tank
$T_{v,w}$	K	temperature of the vapour on the working fluid side
$T_{v,sol}$	K	temperature of the vapour on the solution side
p_w	bar	pressure in the working fluid tank
p_{sol}	bar	pressure of the solution
h_w	$\frac{kJ}{kg}$	specific enthalpy of the working fluid
h_{sol}	$\frac{kJ}{kg}$	specific enthalpy of the solution
$h_{v,w}$	$\frac{kJ}{kg}$	specific enthalpy of the vapour on the working fluid side
$h_{v,sol}$	$\frac{kJ}{kg}$	specific enthalpy of the vapour on the solution side
X_{salt}	$\frac{kg\,salt}{kg\,sol}$	mass concentration of salt in the solution
m_{flow}	$\frac{kg}{s}$	mass flow rate between the two tanks

Table 4: Methods of choice

Solver	**Properties**
ode45	non-stiff, medium order, Runge-Kutta method (Dormand-Prince)
	4^{th} - 5^{th} order, MATLAB [45]
ode15i	implicit, variable order, BDF, MATLAB [46]
DASSL	implemented in Dymola, BDF (adapted from [51]), variable step-size
GENDA	DAE, BDF (adapted from DASSL of [51])
	or Runge-Kutta (adapted from RADAU5 of Hairer/Wanner [62])

5 Numerical Solution

In this section, we apply the preceding results to simulate the discharge model (2.1). We compare the performance of several numerical solvers applied to the original DAE (2.1) as well as to the semi-explicit reformulation (4.1), (4.2), cp. Table 4.
For the original DAE (2.1), we compare the solver DASSL [51] based on BDF methods [15, 24] and the solver GENDA [40] using either BDF or Runge-Kutta methods [7, 24]. To investigate the effect of the semi-explicit reformulation onto the performance of a numerical solver, we apply these DAE solvers to the semi-explicit reformulation (4.1), (4.2) and compare the results with the numerical solution of the original system (2.1).
Due to the semi-explicit structure, the reformulation (4.1), (4.2) admits to apply explicit ODE solver, i.e., discretizing the differential equation (4.1) using an explicit solver, the obtained approximation can be used to evaluate the algebraic equation (4.2). We choose *ode45*, a medium order Runge-Kutta method based on Dormand-Prince for non-stiff explicit ODEs [45], and *ode15i*, a variable order BDF method solver for implicit ODEs and strangeness-free DAEs [46] for this task and compare its performance with DASSL and GENDA.
Note that using *ode15i*, even though this solver is designed for fully implicit differential equations, failed on the discretization of the original DAE (2.1) as the Newton method does not converge.

In order to compare the performance of the solvers, we consider two different cases from the plausibility analysis in [64] differing in the initial solution mass $m_{sol,0}$. As the reference case we assume as examplary value $m_{sol,0} = 3$ kg. As a quasi-steady-state scenario, we assume $m_{sol,0} = 243$ kg. Choosing an increased initial solution mass results in a significantly smaller concentration change during the discharge step since the evaporation of $1kg$ water given in both cases has relatively less effect on an increased solution mass. This provokes nearly time constant quantities, a so called quasi-steady-state behavior of the system. Numerically, the effect of decreased initial slopes may have an effect.
To evaluate the thermodynamic property functions $f_1, ..., f_8$, cp. Table 1, we use the property libraries provided by [30] and [50] implemented in Modelica and MATLAB [26].
For the initial conditions, we assume the initial temperatures and masses in the tanks to be given and the initial concentration of the solution. These values are physically more reasonable design parameters than the differential variables of the original DAE (2.1). The remaining initial values can be calculated from the above mentioned as shown in equation (4.7). Given x_0, then $\dot{x}_0$ can be computed directly using the semi-explicit reformulation (4.2) and (4.1) as explained in Section 4.1.

The performance of the different solvers is illustrated in the Figures 5.1 to 5.16 considering

exemplarily the mass flow rate m_{flow}, concentration X_{salt}, turbine power P_m and the deviation from mass conservation, i.e. the difference $(m_{sol} + m_w) - (m_{sol,0} + m_{w,0})$. The reference case with initial conditions chosen as in (4.7) is shown in Figures 5.1 to 5.8. The quasi-steady-state case with a strongly increased initial solution mass of $m_{sol,0} = 243$ kg is shown in Figures 5.9 to 5.16. The relative errors of the considered quantities using the numerical solution obtained by DASSL as reference are shown in Figures 5.17 to 5.28.
For the reference and the quasi-steady state case we observe that the DAE solvers DASSL and GENDA applied to the original DAE are better off regarding the simulation time than the semi-explicit solution of the semi-explicit reformulation since the algebraic loop takes a very long time compared to the other results. The lower accuracy of the DASSL solver compared to GENDA is physically irrelevant and is compensated by factor 10-20 faster simulation, cp. Table 5.

Description of the results

We describe the numerical deviations since the physical plausibility of the results from Dymola has already been discussed on a qualitatively in [64, p. 31ff.].
The oscillation of the DASSL solution in the depicted accuracy range in the Figures 5.4 and 5.12 leads to dominantly blue (or black) plots. This behaviour is confirmed by Table 5 indicating a higher algebraic acccuracy of the solver GENDA compared with the simple DASSL. Figure 5.5 shows an oscillation in the mass flow rate in the solution of the ODE system for ode15i. The oscillations in the Figures 5.8 and 5.16 show ode45 as the ODE solver with lowest numerical accuracy in the range of 10^{-13}. The relative errors shown in the Figures 5.17 to 5.28 with the DASSL solution as reference show that the results of ODE and DAE solvers have similar time curves while no correlation seems to exist between the errors of the same variables in the reference and the quasi-steady-state case. The errors of ode45 show oscillations whose average is following the lines of the errors of GENDA and ode15i.
The error of the mass flow rate in both cases and of the turbine power in the quasi-steady-state case has its maximum at $t = 0$. The concentration in the quasi-steady-state case and the turbine power in the reference case show an increasing error. Further, there is strong oscillations in the ODE error for the reference case while the quasi-steady-state case shows less oscillations. The largest error of nearly 2% is reached by the turbine power of the GENDA solver solving the original DAE system (Figure 5.19).
Table 5 shows that DASSL is the fastest solver followed by GENDA, i.e. the DAE solvers are faster than the ODE solvers, even only for the differential part. The algebraic loop takes most time and differs according to the solver. [2]

Analysis of the results

As a result of the comparison, we can state that in terms of simulation time, DAE solvers are to be prefered. Dependent on the needed accuracy which seems to be high enough in the case of DASSL, either DASSL or GENDA should be chosen (cp. Table 5). The semi-explicit reformulation does not bring an advantage with respect to simlation time or accuracy but can be interesting when the initial conditions are not that easily choosable.

[2] Please note that the simulation time is dependent on the computing capacity. In order to get comparable numbers, the same computer has been used for all simulations except for the algebraic part of GENDA in the reference case. But the orders of magnitude are clearly comparable and the analysis is not corrupted by this fact.

Table 5: Simulation results of the discharge step for the reference case (ref) and quasi-steady-state case (qss) from [64]: simulation time (differential part (d), algebraic part (a)) and range of mass conservation

System	**Solver**	**Simulation Time**		**Range of mass conservation**	
		ref	qss	ref	qss
original (2.1)	DASSL	0.4 s	0.5 s	10^{-7}	10^{-6}
	GENDA	7.0 s	5.2 s	10^{-15}	10^{-13}
semi-exp.(4.1), (4.2)	ode45	d: 15.3 s a: 297.5 s	d: 5.9 s a: 302.4 s	10^{-13}	10^{-12}
	ode15i	d: 37.9 s a: 303.3	d: 6.4 s a: 311.6 s	10^{-13}	10^{-12}
	GENDA	d: 59.2 s a: 233.7 s	d: 15.7 s a: missing	10^{-15}	10^{-12}

Higher errors at $t = 0$ s in case of the mass flow rate and the turbine power in the quasi-steady-state case may be explained by the different way the initial conditions are treated. While the DASSL solution starts with the Dymola inherent way of treating the initial conditions, for all other cases the initial conditions are analytically calculated as described in Section 4.1.
Comparing the reference and the quasi-steady-state case, we find that the error calculation follows no pattern. This may be the reason because the DASSL solver in Dymola may be the least accurate and not suitable to be chosen as reference.
The following aspects have led to difficulties for all the solvers: the square root in equation (2.1p), stiffness, property functions which only work in a specific range of input variables (see Table 1). Therefore, the careful choice of the stepsize is a crucial factor for possible reduction of simulation time. Its influence on the numerical performance should be investigated in further research.

We have seen that the discharge model equations of the Honigmann process are strangeness-free and can be simulated as a whole using the DASSL solver in Dymola and the DAE solver GENDA [40] based on a modified DASSL. Solving the semi-explicit reformulation of the model equations with the MATLAB solvers ode45, ode15i and GENDA does give similar results but needs more time since the algebraic part is evaluated separately.

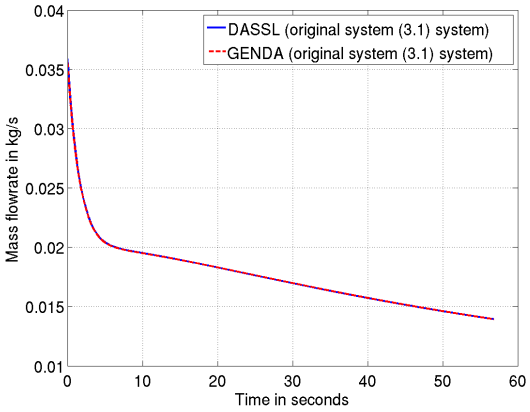

Figure 5.1: Mass flow rate ($m_{sol,0} = 3$ kg)

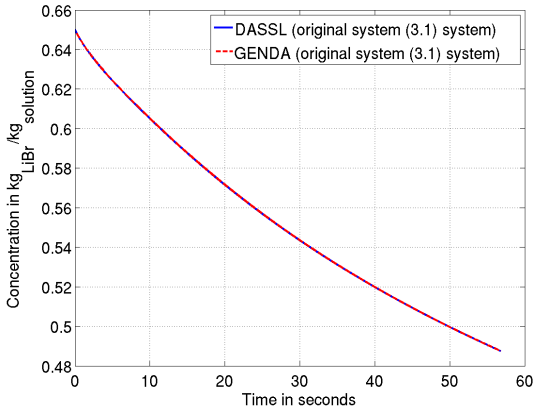

Figure 5.2: Concentration ($m_{sol,0} = 3$ kg)

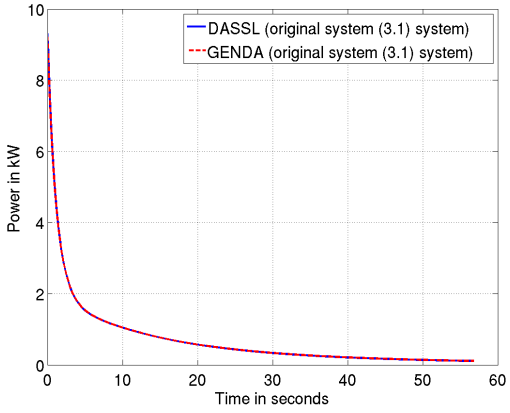

Figure 5.3: Power ($m_{sol,0} = 3$ kg)

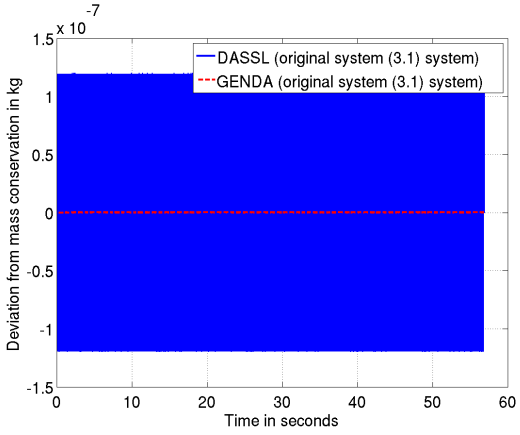

Figure 5.4: Mass conservation ($m_{sol,0} = 3$ kg)

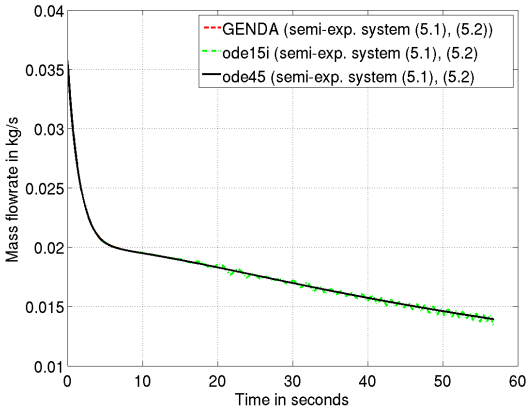

Figure 5.5: Mass flow rate ($m_{sol,0} = 3$ kg)

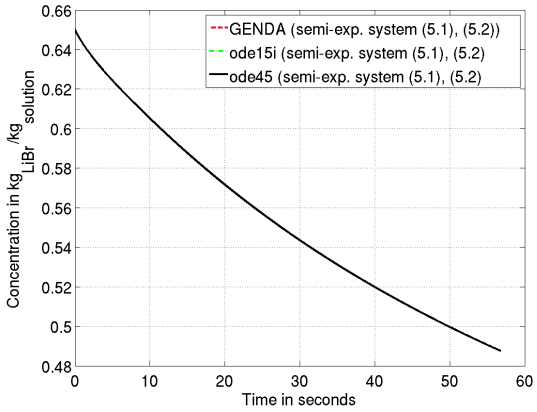

Figure 5.6: Concentration ($m_{sol,0} = 3$ kg)

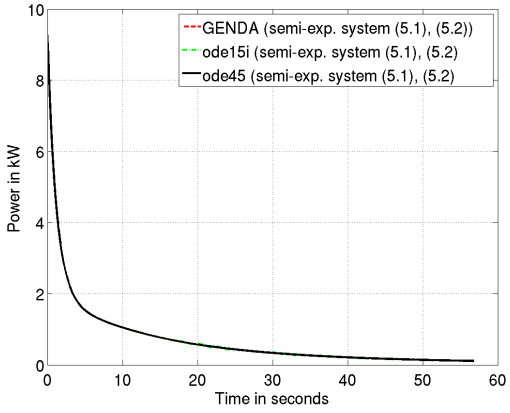

Figure 5.7: Power ($m_{sol,0} = 3$ kg)

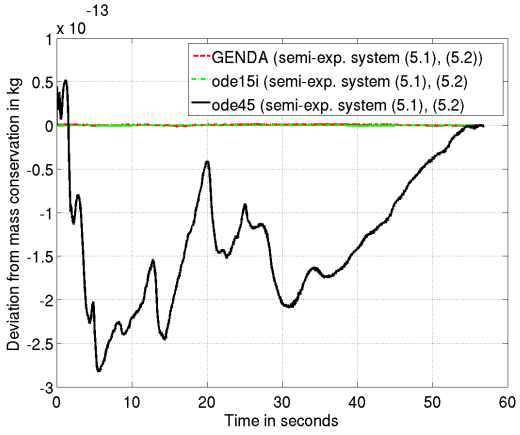

Figure 5.8: Mass conservation ($m_{sol,0} = 3$ kg)

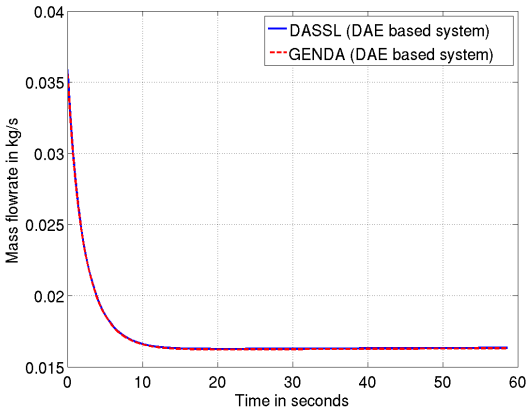

Figure 5.9: Mass flow rate ($m_{sol,0} = 243$ kg)

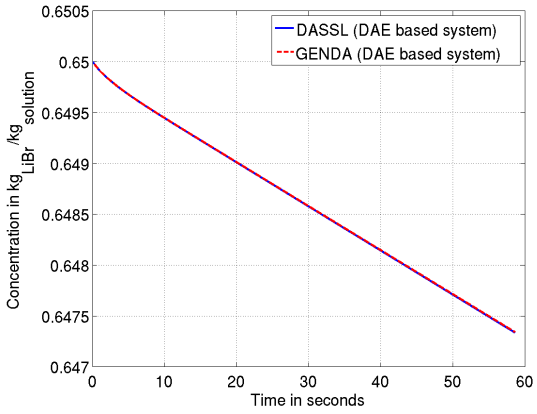

Figure 5.10: Concentration ($m_{sol,0} = 243$ kg)

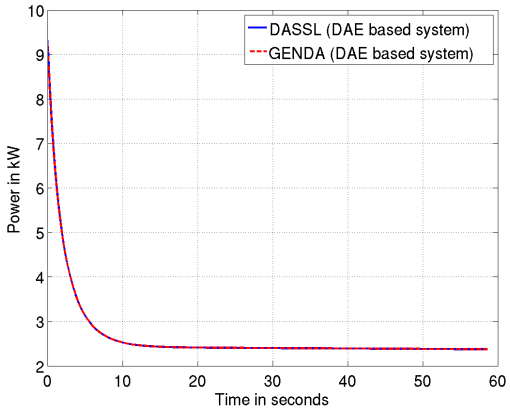

Figure 5.11: Power ($m_{sol,0} = 243$ kg)

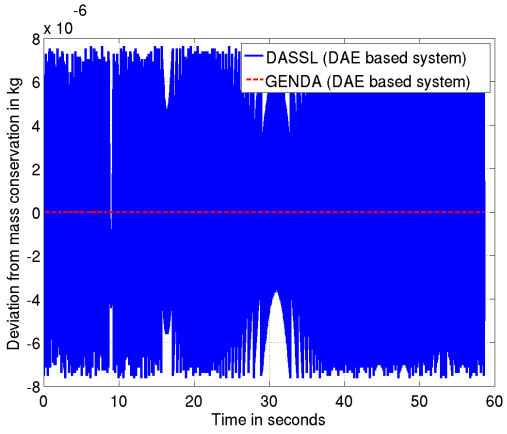

Figure 5.12: Mass conservation ($m_{sol,0} = 243$ kg)

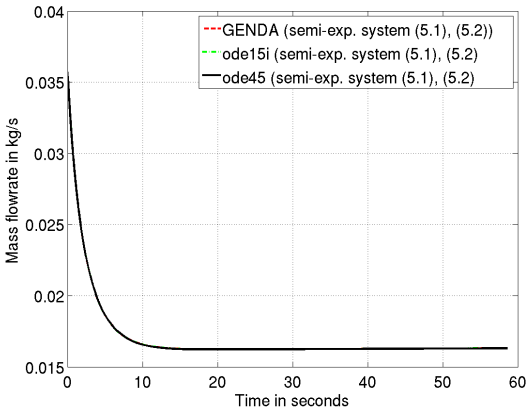

Figure 5.13: Mass flow rate ($m_{sol,0} = 243$ kg)

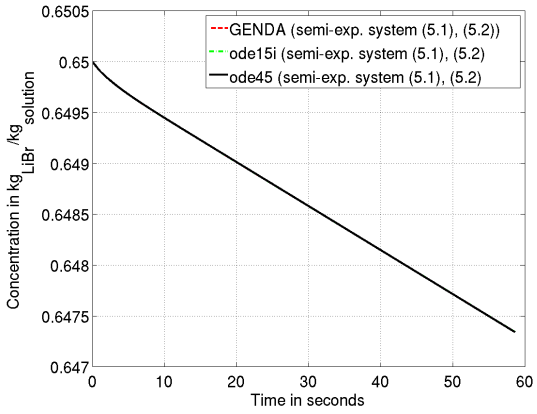

Figure 5.14: Concentration ($m_{sol,0} = 243$ kg)

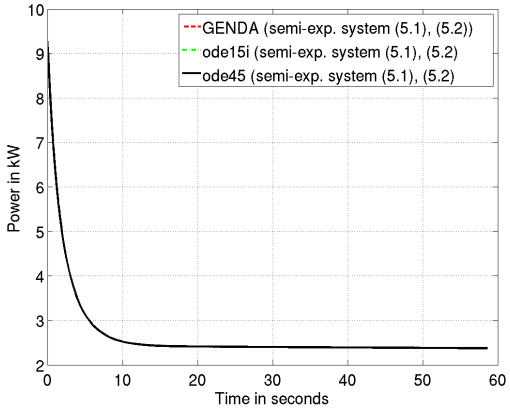

Figure 5.15: Power ($m_{sol,0} = 243$ kg)

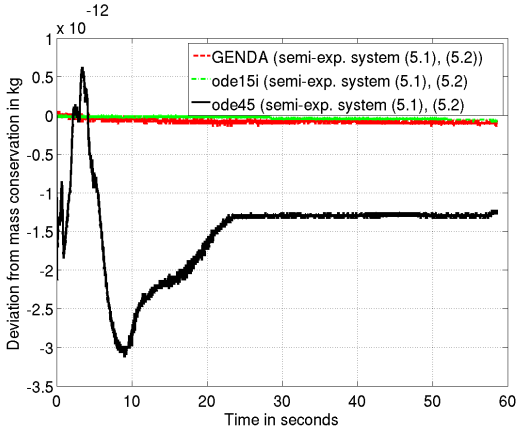

Figure 5.16: Mass conservation ($m_{sol,0} = 243$ kg)

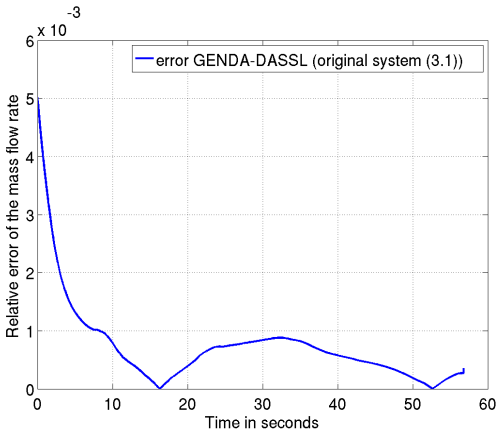

Figure 5.17: Mass flow rate - error ($m_{sol,0} = 3$ kg)

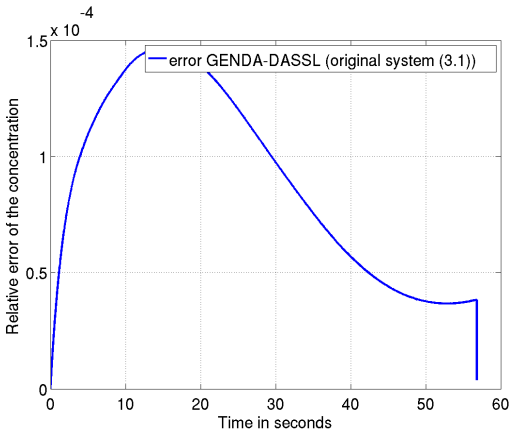

Figure 5.18: Concentration - error ($m_{sol,0} = 3$ kg)

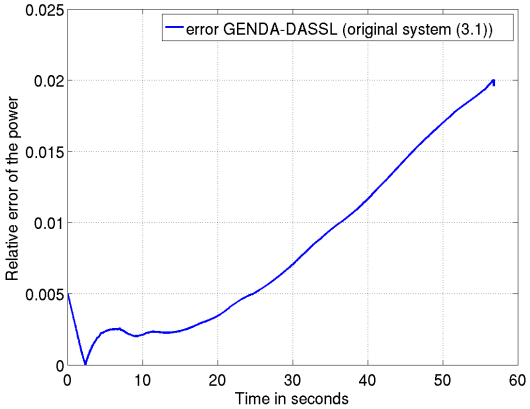

Figure 5.19: Power - error ($m_{sol,0} = 3$ kg)

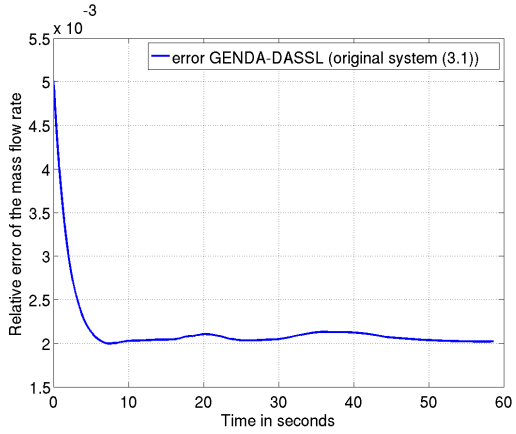

Figure 5.20: Mass flow rate - error ($m_{sol,0} = 243$ kg)

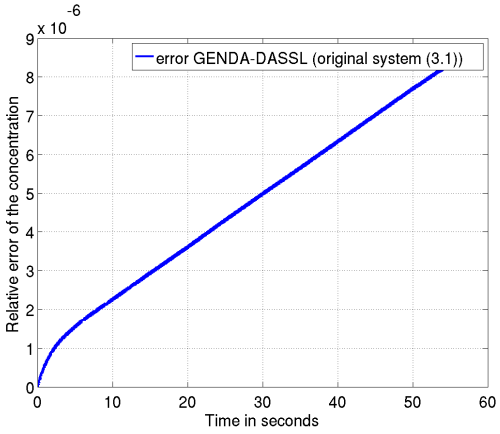

Figure 5.21: Concentration - error ($m_{sol,0} = 243$ kg)

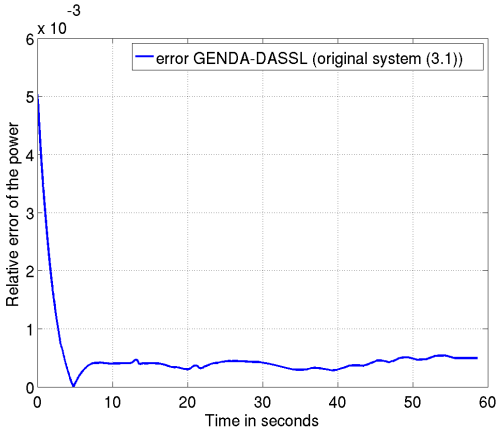

Figure 5.22: Power - error ($m_{sol,0} = 243$ kg)

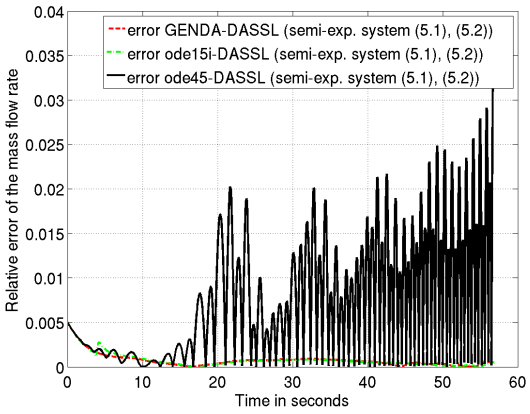

Figure 5.23: Mass flow rate - error ($m_{sol,0} = 3$ kg)

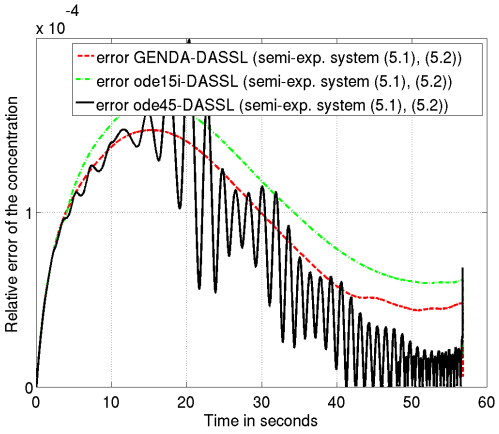

Figure 5.24: Concentration - error ($m_{sol,0} = 3$ kg)

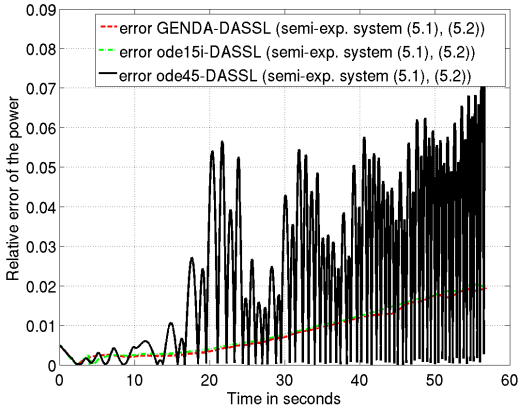

Figure 5.25: Power - error ($m_{sol,0} = 3$ kg)

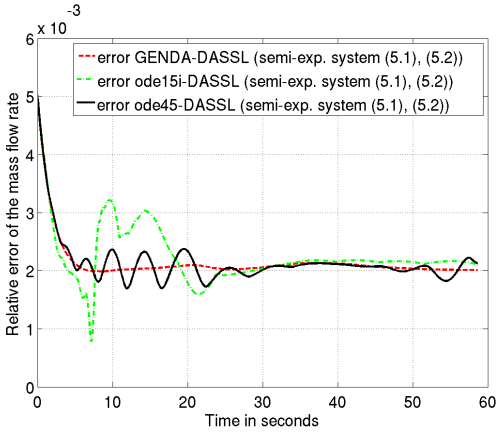

Figure 5.26: Mass flow rate - error ($m_{sol,0} = 243$ kg)

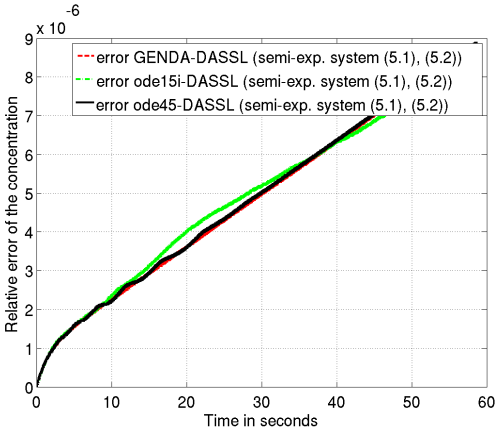

Figure 5.27: Concentration - error ($m_{sol,0} = 243$ kg)

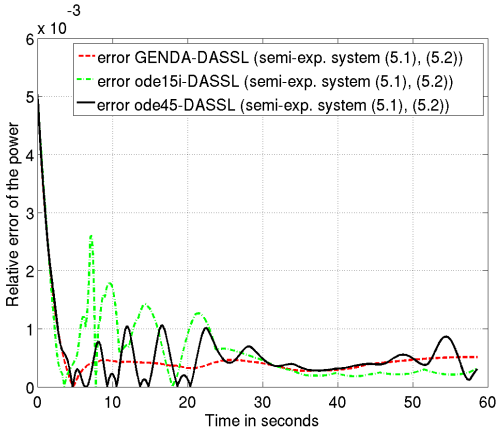

Figure 5.28: Power - error ($m_{sol,0} = 243$ kg)

6 Conclusion and further research

We have studied the Honigmann model as derived in [64] with respect to the (unique) solvability. Using the framework of the strangeness-index, we have identified the model describing the discharging step as a strangeness-free and regular DAE, hence, as a DAE possessing a unique solution for every consistent initial value. We have specified the domain of definition of this model as that set of stages for which there exists a pressure difference between the solution and the water tank. Using the Moore-Penrose remodeling of the system, we have verified that the DAE model is positive, i.e., reflects the physical property of componentwise nonnegative solutions. We have compared the performance of several DAE and ODE solvers for the discharging model and its semi-explicit reformulation.
For the charging model, we have discovered that the system lacks an equation for the mass flow, hence does not necessarily specify a unique solution for every consistent initial value. Further research is needed in order to construct a strangeness-free remodeling using either the concept of the strangeness-index or a physically motivated remodeling of the system.
Given uniquely solvable DAE models for each step of the process, the operation of the storage can be simulated as a whole, allowing to study its performance as well as its energy efficiency.

References

[1] *Proceedings of the 8th International Renewable Energy Storage Conference and Exhibition*, 2013.

[2] Hans Dieter Baehr and Stephan Kabelac. *Thermodynamik*. Springer-Verlag, 2009.

[3] A.K. Baum. *A flow-on-manifold formulation of differential-algebraic equations. Application to positive systems.* PhD thesis, Technische Universität Berlin, Str. des 17. Juni 136, 10623 Berlin, DE, 2014.

[4] A.K. Baum. *A flow-on-manifold formulation of differential-algebraic equations. Application to positive systems.* PhD thesis, Technische Universität Berlin, Str. des 17. Juni 136, 10623 Berlin, DE, 2014.

[5] F. Bornemann and P. Deuflhard. *Numerische Mathematik II.* de Gruyter, Berlin, 2002.

[6] K.E. Brenan, S.L. Campbell, and L.R. Petzold. *Numerical Solution of Initial-Value Problems in Differential-Algebraic Equations.* SIAM Publications, Philadelphia, PA, 2nd edition, 1996.

[7] J.C. Butcher. *The Numerical Analysis of Ordinary Differential Equations: Runge-Kutta and General Linear Methods.* Wiley, Chichester, UK, 1987.

[8] S. L. Campbell. One canonical form for higher index linear time varying singular systems. *Circuits Systems and Signal Processing*, 2:311–326, 1983.

[9] S. L. Campbell. The numerical solution of higher index linear time-varying singular systems of differential equations. *SIAM J. Sci. Statist. Comput.*, 6:334–338, 1985.

[10] S. L. Campbell. High index differential algebraic equations. *J. Mech. of Struct. Mach.*, 23:199–222, 1995.

[11] S. L. Campbell. Linearization of DAEs along trajectories. *Z. Angew. Math. Phys.*, 46(1):70–84, 1995.

[12] S.L. Campbell. *Singular Systems of Differential Equations I.* Pitman, San Francisco, CA, 1980.

[13] S.L. Campbell. *Singular Systems of Differential Equations II.* Pitman, San Francisco, CA, 1982.

[14] S.L. Campbell and C.W. Gear. The index of general nonlinear DAEs. *Numer. Math.*, 72:173–196, 1995.

[15] G. Dahlquist. Convergence and stability in the numerical integration of ordinary differential equations. *Math. Scand.*, 4:33–53, 1956.

[16] E. Eich-Soellner and C. Führer. *Numerical Methods in Multibody Dynamics.* European Consortium for Mathematics in Industry. Teubner Verlag, Stuttgart, DE, 1998.

[17] D. Estévez Schwarz and C. Tischendorf. Structural analysis of electric circuits and consequences for MNA. *Internat. J. Circ. Theor. Appl.*, 28(2):131–162, 2000.

[18] C.W. Gear. Simultaneous numerical solution of differential-algebraic equations. *IEEE Trans. Circ. Theor.*, CT-18:89–95, 1971.

[19] C.W. Gear. Maintaining solution invariants in the numerical solution of ODEs. *SIAM J. Sci. Statist. Comput.*, 7:734–743, 1986.

[20] C.W. Gear. Differential-algebraic equation index transformations. *SIAM J. Sci. Statist. Comput.*, 9:39âĂŞ47, 1988.

[21] C.W. Gear. Differential-algebraic equations, indices, and integral equations. *SIAM J. Numer. Anal.*, 27:1527âĂŞ1534, 1990.

[22] E. Griepentrog and R. März. *Differential-Algebraic Equations and their numerical treatment.* Teubner-Verlag, Leipzig, 1986.

[23] E. Hairer, C. Lubich, and M. Roche. *The Numerical Solution of Differential-Algebraic Systems by Runge-Kutta Methods.* Springer Verlag, Berlin, 1989.

[24] E. Hairer, S.P. Noersett, and G. Wanner. *Solving Ordinary Differential Equations I: Nonstiff Problems.* Springer Verlag, Berlin, 2nd edition, 1993.

[25] E. Hairer and G. Wanner. *Solving Ordinary Differential Equations. II. Stiff and Differential-Algebraic Problems.* Springer Verlag, Berlin, 2nd edition, 1996.

[26] Magnus Holmgren. XSteam for MATLAB. Technical report, MATLAB, 2006.

[27] Moritz Honigmann. Storing power, 1885.

[28] Moritz Honigmann. Method of driving steam-engines, 1886.

[29] W. Hundsdorfer and J. G. Verwer. *Numerical Solution of Time-Dependent Advection-Diffusion-Reaction Equations.* Springer Verlag, Berlin, 2003.

[30] IAPWS. Revised Release on the IAPWS Industrial Formulation 1997 for the Thermodynamic Properties of Water and Steam. `www.iapws.org`, [04.08.2011], August 2007. International Association for the Properties of Water and Steam.

[31] Anna Jahnke. Re-evaluation of the Honigmann-Process: thermo-chemical heat store for the supply of electricity and refrigeration. In *Proceedings of the Heat Powered Cycles Conference, 7. - 9. September, 2009, Berlin, Germany*, 2009.

[32] Anna Jahnke, Lia Strenge, Christian Fleßner, Niklas Wolf, Tim Jungnickel, and Felix Ziegler. First cycle simulations of the Honigmann process with LiBr/H2O and NaOH/H2O as working fluid pairs as a thermochemical energy storage. *International Journal of Low-Carbon Technologies*, 8:i55–i61, July 2013.

[33] Tim Jungnickel. Modellierung des Honigmann-Prozesses als Energiespeicher für die Nutzung von Wärme zur Produktion mechanischer Arbeit. Bachelor's thesis, Technische Universität Berlin, 2011.

[34] J. Kestin. Ein Beitrag zu Stodolas Kegelgesetz. *Wärme- und Stoffübertragung*, 16:53–55, 1982.

[35] P. Kunkel and V. Mehrmann. Canonical forms for linear differential-algebraic equations with variable coefficients. *J. Comput. Appl. Math.*, 56:225–251, 1994.

[36] P. Kunkel and V. Mehrmann. Local and global invariants of linear differential algebraic equations and their relation. *Electr. Trans. Numer. Anal.*, 4:138–157, 1996.

[37] P. Kunkel and V. Mehrmann. Regular solutions of nonlinear differential-algebraic equations and their numerical determination. *Numer. Math.*, 79:581–600, 1998.

[38] P. Kunkel and V. Mehrmann. *Differential-Algebraic Equations. Analysis and Numerical Solution*. EMS Publishing House, Zürich, CH, 2006.

[39] P. Kunkel and V. Mehrmann. Stability properties of differential-algebraic equations and spin-stabilized discretizations. *Electronic Transactions on Numerical Analysis*, 26:385–420, 2007.

[40] P. Kunkel, V. Mehrmann, and I. Seufer. GENDA: A software package for the solution of GEneral Nonlinear Differential-Algebraic equations. Technical Report 730-02, Institut für Mathematik, TU Berlin, D-10623 Berlin, FRG, 2002.

[41] R. Lamour, R. März, and C. Tischendorf. *Differential-Algebraic Equations: A Projector Based Analysis: A Projector Based Analysis*. Differential-Algebraic Equations Forum. Springer, Heidelberg, DE, 2013.

[42] R. März. The index of linear differential algebraic equations with properly stated leading terms. *Results Math.*, 42:308–338, 2002.

[43] R. März. Solvability of linear differential algebraic equations with properly stated leading terms. *Results Math.*, 45(1-2):88–105, 2004.

[44] R. März. Characterizing differential algebraic equations without the use of derivative arrays. *Computers & Mathematics with Applications*, 50(7):1141–1156, 2005.

[45] MathWorks. Mathworks - documentation center, 2014. [Online; accessed 9-August-2014].

[46] MathWorks. Mathworks - documentation center, 2014. [Online; accessed 9-August-2014].

[47] Michael J. Moran and Howard N. Shapiro. *Fundamentals of Engineering Thermodynamics*. Moran, Michael J. and Shapiro, Howard N., 2006.

[48] J.M. Ortega and W.C. Rheinboldt. *Iterative Solution of Nonlinear Equations in Several Variables*. Classics in Applied Mathematics. Society for Industrial and Applied Mathematics, Philadelphia, PA, 2000.

[49] C.C. Pantelides. The consistent initialization of differential-algebraic systems. *SIAM J. Sci. Statist. Comput.*, 9:213–231, 1988.

[50] J. Pátek and J. Klomfar. A computationally effective formulation of the thermodynamic properties of LiBr-H2O solutions from 273 to 500 K over full composition range. *International Journal of Refrigeration*, 29:566–578, 2006.

[51] L. R. Petzold. A description of DASSL. A differential/algebraic system solver. *IMACS Trans. Scientific Computing*, 1:pages 65–68, 1983.

[52] L.R. Petzold. Differential/algebraic equations are not ODEs. *SIAM J.Sci.Statist.Comput.*, 3:367–384, 1982.

[53] J. Pryce. A simple structural analysis method for DAEs. *BIT*, 41:364–394, 2001.

[54] P.J. Rabier and W.C. Rheinboldt. *Theoretical and Numerical Analysis of Differential-Algebraic Equations*, volume VIII of *Handbook of Numerical Analysis*. Elsevier Publications, Amsterdam, Netherlands, 2002.

[55] W.C. Rheinboldt. Differential-algebraic systems as differential equations on manifolds. *Mathematics of computation*, 43(168):473–482, 1984.

[56] R. Riaza and R. März. Linear differential-algebraic equations with properly stated leading terms: Regular points. *J. Math. Anal. Appl.*, 323:1279–1299, 2006.

[57] R. Riaza and R. März. A simpler construction of the matrix chain defining the tractability index of linear DAEs. *Appl. Math. Letters*, 21:326–331, 2008.

[58] R. E. Roberson and R. Schwertassek. *Dynamics of multibody systems*, volume 18. Springer, Heidelberg, DE, 1988.

[59] Irm Scheer-Pontenagel and Corinna Kolks. Editorial to the proceedings of the 8th international renewable energy storage conference and exhibition (IRES 2013). *Energy Procedia*, 46:1:2, 2013.

[60] W. O. Schiehlen. *Multibody systems handbook*, volume 6. Springer, Heidelberg, DE, 1990.

[61] W. O. Schiehlen. Multibody system dynamics: roots and perspectives. *Multibody system dynamics*, 1(2):149–188, 1997.

[62] Springer-Verlag, editor. *Solving Ordinary Differential Equations II*. E. Hairer and G. Wanner, 1991.

[63] M. Sterner and I. Stadler. *Energiespeicher - Bedarf, Technologien, Integration.* Springer-Verlag, 2014.

[64] Lia Strenge. Der Honigmann-Prozess als thermochemischer Energiespeicher zur Erzeugung mechanischer Arbeit aus Niedertemperaturwärme - Modellierung und Simulation in Modelica. Bachelor thesis, Technische Universität Berlin, 2011.

[65] C. Tischendorf. Topological index calculation of differential-algebraic equations in circuit simulation. *Surv. Math. Ind.*, 8:187–199, 1999.